

55p ref Submitted for Publication

UNPUBLISHED PRELIMINARY DATA

1 The Non-Existence of Quiescent Plasma States in Ion Propulsion*

→ Heinrich Derfler
Stanford Electronics Laboratories
Stanford University
Stanford, California

N65-82171

Code Note

8299000

The problem of neutralizing an ion beam is analyzed within the framework of a one-dimensional collision-free theory. The character of steady state solutions obtained depends upon the ratio between the mean thermal speed of the electrons and the ion velocity. When the ions are faster, excess electrons are returned to their source from a finite distance behind the electron emitter and the flow of charges is unidirectional (beam like) further downstream. When the electrons are faster, a "floating target" must be postulated downstream to intercept electrons and ions at equal rates and to return excess electrons to the emitter. In this case the flow pattern of the electrons is 'plasma like'. Both beam-like and plasma-like states are found to be unstable with respect to small perturbations. Thus the plasma driving a space vehicle cannot be in a quiescent state.

FACILITY FORM 802

(ACCESSION NUMBER)	(THRU)
55	
(PAGES)	(CODE)
CR-55137	
(NASA CR OR TMX OR AD NUMBER)	(CATEGORY)

~~AVAILABILITY TO THE PUBLIC~~

* Work supported by the National Aeronautics and Space Administration under (NASA Grant Nsg-299-63)

Reprints available

UNPUBLISHED PRELIMINARY DATA

**"The Non Existence of Quiescent Plasma
States in Ion Propulsion"**

by

Heinrich Derfler

Stanford Electronics Laboratories

Stanford University
Stanford, California

NSG-299

~~ALL INFORMATION CONTAINED HEREIN IS UNCLASSIFIED~~

CONTENTS

Abstract

I	Introduction	p. 1
II	Velocity Distribution Functions and their Moments	p. 4
III	Conditions for Charge Neutrality	p. 11
IV	The Pressure Balance	p. 15
V	Plasma-like States $\langle v_- \rangle > v_+$	p. 17
VI	Beam-like States $\langle v_- \rangle < v_+$	p. 21
VII	Stability Analysis	p. 25
VIII	Summary of Conclusions	p. 30
	Acknowledgements	p. 31
	Appendix A: Series Representation of Charge and Pressure Functions	p. 32
	Appendix B: Evaluation of Dispersion Integral	p. 34
	References	
	Figures	

11267
ABSTRACT

The problem of neutralizing an ion beam is analyzed within the framework of a one-dimensional collision-free theory. The character of steady state solutions obtained depends upon the ratio between the mean thermal speed of the electrons and the ion velocity.

When the ions are faster, excess electrons are returned to their source from a finite distance behind the electron emitter and the flow of charges is unidirectional (beam like) further downstream.

When the electrons are faster, a "floating target" must be postulated downstream to intercept electrons and ions at equal rates and to return excess electrons to the emitter. In this case the flow pattern of the electrons is 'plasma like'.

Both beam-like and plasma-like states are found to be unstable with respect to small perturbations. Thus the plasma driving a space vehicle cannot be in a quiescent state. *Further*

I. INTRODUCTION

The success of ion propulsion for space vehicles depends on a positive solution of the problem of neutralization. Unless electrons and ions merging from the nozzle of the space ship at equal rates mix to form a neutral plasma, these charges are returned by static fields building up behind the vehicle.

The single most important parameter characterizing the state of the emerging plasma turns out to be the ratio between the mean thermal speed of the emitted electrons and the exhaust velocity of the ions,

$$\sigma = \langle |v_-| \rangle / v_+ \quad (1)$$

The limiting cases of very cold and very hot electrons have been discussed extensively in the literature^{1,2,3}.

In the limit $\sigma \rightarrow 0$ the electrons may be treated like a beam of initial velocity $v_- = \langle |v_-| \rangle$ and their density q_- is uniquely determined by the current j_- of the electron beam launched into the ion stream

$$q_- = j_- / v_- \quad (2)$$

Space periodic potential distributions which have been obtained in this case^{1,2} are characterized by rather arbitrary assumptions on the electric field at the injection plane of the electrons.

In the limit $\sigma \rightarrow \infty$ the electrons may be treated as a complete plasma and the scale height law based on a local Maxwell distribution of velocities is generally assumed to hold for the electron density:

$$q_- = q \exp(-e\phi/kT_-) \quad (3)$$

Steady state solutions obtained in this case lack an explanation of exactly how a local Maxwell distribution of electron velocities is established³.

In general the exhaust velocity of the ions v_+

is fixed by an optimizing procedure involving the components of the space vehicle and the length of its mission⁴. For cesium ions and electrons originating from a tungsten emitter the parameter σ is thus pretty well confined to a region near unity in which neither the scale height law nor the equations of beam dynamics hold for the electrons. It is the purpose of this paper to obtain steady state solutions in this transition region and to investigate their stability against small perturbations.

The method of investigation is based on discontinuous velocity distributions obtained from the one-dimensional, time-independent Boltzmann equation for preconceived potential distributions. These velocity distribution functions are required to match Gauss distributions at the emitters and to comply with the space charge equation. An element which is extraneous to the concept of a plasma in free space has to be postulated for the consistency of these solutions, namely a "floating target" or equivalent mechanism for recombination of charges. The self-consistent potential distributions thus obtained are not the only ones possible; however, certain ambiguities such as those discussed above in the limiting cases $\sigma \rightarrow 0$ and $\sigma \rightarrow \infty$ do not arise. Data obtained for three different designs $\sigma = 2, 1, 1/2$ of an ion motor are collected in Table I.

Finally the stability of these distribution functions is tested by investigating the dispersion relation for small perturbations in regions of nearly uniform potential. All the D.C. solutions obtained are found to be unstable within the framework of the one-dimensional theory presented.

II. THE VELOCITY DISTRIBUTION FUNCTIONS AND THEIR MOMENTS

A schematic outline of an ion motor is shown in Fig. 1. Corresponding diagrams of potential versus distance are shown in Figs. 2(a) and 3(a). Ions emitted from the anode pass through the accelerator grid c_1 and the electron emitting grid c . A small bias applied to the electron emitter is sufficient to prevent electrons from interfering with the operation of the ion gun $a < x < c_1$. A larger bias may be used to incorporate an Accel.-Decel. system into the design, allowing for larger electrode spacings. Enough electrons are supposed to be supplied such that the electron emitter is positive with respect to its immediate surroundings. A potential minimum is thus formed at $x = c_2$ behind the ion motor. Whether it is an absolute minimum as in Fig. 2(a) or a relative minimum as in Fig. 3(a) depends on whether the mean thermal speed of the electrons is larger or smaller than the ion exhaust velocity, as will be found in due course. In an actual space environment no net current can be drawn from the ion motor. To simulate this condition in an experimental setup, a floating target⁵, intercepting and recombining electrons and ions at equal rates, is placed at a position $x = c_2$ in Fig. 2(a) or any position $x > c_2$ in Fig. 3(a). The redundancy of this target and the self-consistency of these potential distributions are the subject of this study. Alternative potential distributions,

allowing for large charge separations, such as those shown in Fig. 2(a) by broken lines will be omitted in this paper.

The velocity distributions $f^{\pm}(v)$ of electrons and ions moving through regions of arbitrary potential are found from Boltzmann's transport equation

$$v \frac{\partial f^{\pm}}{\partial x} \pm \frac{e}{m_{\pm}} E \frac{\partial f^{\pm}}{\partial v} = 0 \quad E = - \frac{d\phi}{dx} \quad (4)$$

We recollect the properties of this differential equation and its solutions:

1) The characteristics are given by the energy integral

$$\frac{1}{2} m_{\pm} v^2 \pm e\phi(x) = \frac{1}{2} m_{\pm} v_{\pm}^2(x_0) \pm e\phi(x_0) \quad (5)$$

where $v_{\pm}(x_0)$ and $\phi(x_0)$ are the 'initial velocities' and the potential at a given position $x = x_0$. With a knowledge of the potential distribution $\phi(x)$ the flow lines of electron in v - x phase space can be drawn immediately as shown in Figs. 2(b) and 3(b) and corresponding diagrams could be constructed for ions.

ii) Any function of total energy is a solution of (4), i.e. for electrons,

$$F^-(x, v) = F^-\left(m_- \frac{v^2}{2} - e\phi(x) + e\phi(x_0)\right) \quad (6)$$

iii) If $F_1^-(x, v)$ and $F_2^-(x, v)$ are any two solutions of (4), then also their sum and products are ^{also} solutions of (4)

1v) Let $H(x) = 1/2 (1 + \text{sgn}(x))$ be the unit step function, then by definition

$$H\left(\frac{m_-}{2} - \frac{v^2}{2} - e\phi(x) + e\phi(x_0)\right) = H\left(v - \left(\frac{2e}{m_-}\phi(x) - \frac{2e}{m_-}\phi(x_0)\right)^{1/2}\right) + H\left(-v - \left(\frac{2e}{m_-}\phi(x) - \frac{2e}{m_-}\phi(x_0)\right)^{1/2}\right) \quad (7)$$

is a solution of (4). Not only is the sum of the step functions in (7) a solution of (4) but also each term separately as can be shown immediately by inserting into (4) and using the fact that $dH(x)/dx = \delta(x)$ and $x\delta(x) = 0$.⁶ These solutions demonstrate the fact that discontinuities in the solutions of linear partial differential equations can occur only along characteristics. Step functions are used conveniently to describe the reflection and trapping of particles in potential wells, as for electrons emitted from the cathode c and returned at or before $x = c_2$ in Figs. 2(b) and 3(b).

By combining solutions in the form

$$f^-(x, v) = \sum_v F_v^-(x, v) H\left(v - \left(\frac{2e}{m_-}\phi(x) - \frac{2e}{m_-}\phi(a_v)\right)^{1/2}\right) H\left(v^2 - \left(\frac{2e}{m_-}\phi(x) - \frac{2e}{m_-}\phi(b_v)\right)^{1/2}\right) \dots \quad (8)$$

almost any preconceived idea of what the potential distribution in space should be can be made self-consistent with the space charge equation

$$\epsilon_0 \frac{dE}{dx} = e \int f^+(x, v) dv - e \int f^-(x, v) dv \quad (9)$$

as shown in a paper by Bernstein et al.⁷ To match the boundary conditions in ion engines with assumed d.c. potential variations as shown in Figs. 2(a) and 3(a), we have in particular

the truncated Gaussians

$$f^+(x, v) = n_+(a) \left(\frac{m_+}{2\pi kT_+} \right)^{1/2} \exp \left(- \frac{m_+ v^2}{2kT_+} - \frac{e}{kT_+} \phi(x) + \frac{e}{kT_+} \phi(a) \right) H \left(v + \left(\frac{2e}{m_+} \phi(a_1) - \frac{2e}{m_+} \phi(x) \right)^{1/2} \right), \quad x > a \quad (10)$$

$$f(x, v) = n_-(c) \left(\frac{m_-}{2\pi kT_-} \right)^{1/2} \exp \left(- \frac{m_- v^2}{2kT_-} + \frac{e}{kT_-} \phi(x) - \frac{e}{kT_-} \phi(c) \right) H \left(-v + \left(\frac{2e}{m_-} \phi(x) - \frac{2e}{m_-} \phi(c_1) \right)^{1/2} \right), \quad x < c \quad (11)$$

$$f^-(x, v) = n_-(c) \left(\frac{m_-}{2\pi kT_-} \right)^{1/2} \exp \left(- \frac{m_- v^2}{2kT_-} + \frac{e}{kT_-} \phi(c) \right) H \left(v - \left(\frac{2e}{m_-} \phi(x) - \frac{2e}{m_-} \phi(c_2) \right)^{1/2} \right), \quad x > c \quad (12)$$

where the following sign convention has been adopted and will be used consistently throughout this paper

$$\text{sgn}(\phi(x) - \phi(y))^{1/2} = \text{sgn}(x-y) \quad (13)$$

By this convention the characteristic separating empty from occupied regions in phase space Figs. 2(b) and 3(b) are described most conveniently.

The following assumptions are implied in writing the distribution functions in this form:

1) Both electrons and ions are emitted with a Gaussian distribution of velocities.

ii) The accelerator grid c_1 is transparent to both electrons and ions, which can be achieved by focusing.

iii) The electron emitting grid c is transparent to ions but not to electrons. This implies that electrons emitted from the grid are reabsorbed upon return.

iv) No electrons are trapped in regions such as $c_2 < x < c_3$ in Fig. 3(a) since in the absence of fluctuations or collisions no mechanism is available to fill these traps.

To investigate the self-consistency of the preconceived potential distributions shown in Figs. 2(a) and 3(a) we need to discuss space charge density, current density and kinetic pressure which are given by the first three moments of the distribution functions (10, 11, 12).

$$q(x) = e \int f(x,v)dv, \quad j = e \int vf(x,v)dv, \quad p = m \int v^2 f(x,v)dv \quad (14)$$

These integrations are easily performed in terms of error functions and are conveniently expressed with normalized charge and pressure functions defined by:

$$Q(x) = e^{x^2} \operatorname{erfc}(x) \quad (15)$$

$$P(x) = 2\pi^{-1/2}x + Q(x) \quad (16)$$

A plot of these function is shown in Figs. 4 and 5 together with convenient approximations for large positive and negative values of x . We shall recognize these limits as the beam and plasma limit respectively. A simple approximation $P_1(x)$

$$P(x) \approx P_1(x) \equiv \frac{1 + 1/2 \pi^{1/2} x + x^2}{1 + 1/2 \pi^{1/2} x}, \quad x > -0.6 \quad (17)$$

which bridges the gap between these limits is also shown in Fig. 5. Further mathematical information on these functions is given in appendix A.

In terms of these functions the moments (14) are simply given by:

$$j_+ = j_{s+} \exp \left(\frac{e}{kT_+} \phi(a) - \frac{e}{kT_+} \phi(a_1) \right) \quad x > a \quad (18)$$

$$-j = j_{s-} \exp \left(\frac{e}{kT_-} \phi(c_1) - \frac{e}{kT_-} \phi(c) \right) \quad x < c \quad (19)$$

$$j_- = j_{s-} \exp \left(\frac{e}{kT_-} \phi(c_2) - \frac{e}{kT_-} \phi(c) \right) \quad x > c \quad (20)$$

$$q_+(x) = \frac{j_+}{\langle |v_+| \rangle} Q \left(- \left(\frac{e}{kT_+} \phi(a_1) - \frac{e}{kT_+} \phi(x) \right)^{1/2} \right) \quad x > a \quad (21)$$

$$-q(x) = \frac{-j}{\langle |v_-| \rangle} Q \left(- \left(\frac{e}{kT_-} \phi(x) - \frac{e}{kT_-} \phi(c_1) \right)^{1/2} \right) \quad x < c \quad (22)$$

$$q_-(x) = \frac{j_-}{\langle |v_-| \rangle} Q \left(+ \left(\frac{e}{kT_+} \phi(x) - \frac{e}{kT_+} \phi(c_2) \right)^{1/2} \right) \quad x > c \quad (23)$$

$$p_+(x) = \frac{kT_+}{e} \frac{j_+}{\langle |v_+| \rangle} P\left(-\left(\frac{e}{kT_+} \phi(a_1) - \frac{e}{kT_+} \phi(x)\right)^{1/2}\right) \quad x > a \quad (24)$$

$$p_-(x) = \frac{kT_-}{e} \frac{j_-}{\langle |v_-| \rangle} P\left(-\left(\frac{e}{kT_-} \phi(x) - \frac{e}{kT_-} \phi(c_1)\right)^{1/2}\right) \quad x < c \quad (25)$$

$$p_-(x) = \frac{kT_-}{e} \frac{j_-}{\langle |v_-| \rangle} P\left(+\left(\frac{e}{kT_-} \phi(x) - \frac{e}{kT_-} \phi(c_2)\right)^{1/2}\right) \quad x > c \quad (26)$$

As a matter of convenience, the number densities $n_+(a)$ and $n_-(c)$ have been eliminated from these formulae by use of the saturation current densities $j_{s\pm}$ and the mean thermal speeds $\langle |v_{\pm}| \rangle$ defined by:

$$j_{s+} = 1/2 n_+(a) \langle |v_+| \rangle \quad \langle |v_+| \rangle = \left(\frac{2kT_+}{\pi m_+}\right)^{1/2} \quad (27)$$

$$j_{s-} = 1/2 n_-(a) \langle |v_-| \rangle \quad \langle |v_-| \rangle = \left(\frac{2kT_-}{\pi m_-}\right)^{1/2} \quad (28)$$

III. THE CONDITION FOR CHARGE NEUTRALITY

The design of an ion motor can be split into three parts

- 1) The Ion Gun ($a < x < c_1$).

Within this region the condition

$$e\phi(a_1) - e\phi(x) \gg kT_+, \quad a < x < c_1 \quad (29)$$

holds almost everywhere and the space charge density can be calculated from the asymptotic approximation (A5)

$Q(x) = \pi^{-1/2} x^{-1}$, giving

$$q_+(x) = - \frac{j_+}{\langle |v_+| \rangle} \pi^{-1/2} \left(\frac{e}{kT_+} \phi(a_1) - \frac{e}{kT_+} \phi(x) \right)^{1/2} = \frac{j_+}{v_+(x)} \quad (30)$$

where

$$v_+(x) = - \left(\frac{2e}{m_+} \phi(a_1) - \frac{2e}{m_+} \phi(x) \right)^{1/2} \quad (31)$$

In this limit the temperature of the ions drops out and almost all the ions at a given position x have the same velocity $v_+(x)$ as given by (31).

The gun design based on this beam model is well described in the literature and will not be discussed any further⁸. We quote Langmuir Child's law for planar flow

$$j_+ = \frac{4\epsilon_0}{9} \left(\frac{2e}{m_+} \right)^{1/2} \left(\phi(a_1) - \phi(c_1) \right)^{3/2} (c_1 - a_1)^{-2} \quad (32)$$

Values of current j_+ , voltage $\phi(a_1) - \phi(c_1)$ and distance $c_1 - a_1$ for 3 typical designs are given in table I.

11) The Electron Trap ($c_1 < x < c$).

A positive bias $\phi(c) - \phi(c_1) > 0$ is applied to prevent electrons from reaching the ion gun. In the following we shall assume this bias to be small such that the ion velocity (31) is nearly constant throughout $x > c_1$. This assumption simplifies the algebra considerably but excludes Accel.-Decel. systems from further consideration. We note that the magnitude of the emitter bias essentially does not effect the problem of neutralization and that the following theory can be easily extended to incorporate Accel.-Decel. systems. Since no net current can be drawn from the ion motor into free space we have the condition

$$j_- = j_+ \quad (33)$$

for the down stream electron current. The upstream electron current which manages to escape the trap is given by (19) and for an efficient trap we must have

$$\frac{j_-}{j_+} = \exp \left(\frac{e}{kT_-} \phi(c_1) - \frac{e}{kT_-} \phi(c_2) \right) \equiv \tau \ll 1 \quad (34)$$

To reduce the danger of charge separation and ion reflection such as that associated with the potential diagram shown by the broken line in Fig. 2(a), it is desirable to have a plasma formed within the trap. To establish neutrality we must have

$q_-(b_1) = q_+(b_1)$, $c_1 < b_1 < c$. Thus with equations (22), (30), (34) and $\sigma \approx \langle |v_-| \rangle / v_+(b_1)$ of order unity the following relation is obtained for the plasma potential $\phi(b_1)$:

$$Q \left(- \left(\frac{e}{kT_-} \phi(b_1) - \frac{e}{kT_-} \phi(c_1) \right)^{1/2} \right) = \frac{j_+}{-j} \frac{\langle |v_-| \rangle}{v_+(b_1)} = \frac{\sigma}{\tau} \gg 1 \quad (35)$$

Since the left-hand side is large we can use the 'scale height law' for Q as given by the asymptotic term (A5), $Q = 2 \exp(x^2)$, shown on the left in Fig. 4. Together with (19) the following chain of inequalities is thus obtained.

$$\frac{2j_{s-}}{-j} = 2 \exp \left(\frac{e}{kT_-} \phi(c) - \frac{e}{kT_-} \phi(c_1) \right) > 2 \exp \left(\frac{e}{kT_-} \phi(b_1) - \frac{e}{kT_-} \phi(c_1) \right) = \frac{j_+}{-j} \frac{\langle |v_-| \rangle}{v_+(b_1)} \gg 1 \quad (36)$$

We find that a minimum electron saturation current density

$$j_{s-} > \frac{1}{2} \frac{\langle |v_-| \rangle}{v_+(b_1)} j_+ = \frac{\sigma}{2} j_+ \quad (37)$$

is required to satisfy these conditions.

Values of plasma potentials $\phi(b_1) - \phi(c_1)$ and emitter bias $\phi(c) - \phi(c_1)$ obtained from (36) for a trapping ratio $\tau = 0.01$ and a set of velocity ratios $\sigma = 2, 1, 1/2$ are of the order of several kT_-/e as listed in table I.

For large distances $c - c_1$ between emitter and accelerator grid alternative potential distributions, such as the one shown by the broken line in Fig. 2(a) may become possible. For this particular potential distribution the Ansatz (10) and (11) breaks down and more general distribution functions of the type (8) must be used. These peculiar potential distributions have been discussed in the literature² for the case of cold electrons and ions and are likely to be unstable. An extension of this work to hot electrons and ions is outside the scope of this paper.

111) The Propelling Plasma ($x > c$).

With electrons and ions lost at equal rates from the ion motor, (33), the condition of charge neutrality within the escaping plasma $q_-(b_2) = q_+(b_2)$ becomes, using (23) and (30)

$$Q\left(+\left(\frac{e}{kT_-} \phi(b_2) - \frac{e}{kT_-} \phi(c_2)\right)^{1/2}\right) = \frac{\langle |v_-| \rangle}{v_+(b_2)} \approx \sigma \quad (38)$$

We remember that σ is of order unity as given by economical considerations and therefore neither of the approximations to Q shown in Fig. 4 can be used to invert this equation. The physical

significance of this fact is that neither the 'scale height' law nor the equations of beam dynamics apply in this case. In using a table of $Q(x)$ or the plot in Fig. 4 to solve equation (38) for $\phi(b_2)$, we must keep track of our sign convention (13). Thus if $\sigma > 1$ we have $b_2 < c_2$ as in Fig. 2. If on the other hand, $\sigma < 1$ we have $b_2 > c_2$ as in Fig. 3. Subsequently these two cases will be referred to as 'plasma like' and 'beam like' respectively. For practical values of σ , the plasma potential $\phi(b_2) - \phi(c_2)$ is found to be smaller than kT_-/e as seen in table I.

IV. THE PRESSURE BALANCE

With the charge densities q_{\pm} being known functions of potential ϕ , self-consistency can be established by integrating the space charge equation (9). An integral of this differential equation can be obtained immediately from first principles. Multiplying Boltzmann's Transport equation (4) with vm_{\pm} and integrating over all velocities we have with $f(\pm\infty) = 0$

$$\frac{d}{dx} \int m_{\pm} v^2 f^{\pm}(x, v) dv = \pm E(x) q_{\pm}(x) \quad (39)$$

Adding both equations and using (9) gives

$$\frac{d}{dx} (p_+ + p_-) = E(q_+ - q_-) = \epsilon_0 E \frac{dE}{dx} \quad (40)$$

An integration finally yields the 'pressure balance'

$$\epsilon_0 \frac{E^2}{2} = p_+ + p_- + \text{const.} \quad , \quad E = - \frac{d\phi}{dx} \quad (41)$$

Since the kinetic pressures p_{\pm} are known functions of potential only, the solution of (41), or of Poisson's equation (9), is

$$\left(\frac{\epsilon_0}{2}\right)^{1/2} \int \left(p_+(\phi) + p_-(\phi) + \text{const.}\right)^{-1/2} d\phi = x + \text{const.} \quad (42)$$

Numerical methods must be used to evaluate this integral.

As an example we establish self-consistency within the electron trap $c_1 < x < c$. Introducing kT_-/e and the Debye length λ :

$$\lambda^2 = \epsilon_0 \frac{kT_-}{e} \frac{\langle |v_-| \rangle}{j_-} = \epsilon_0 \frac{kT_-}{eq_-(c_2)} \quad (43)$$

as scaling parameters we define

$$\eta(x) = \frac{e}{kT_-} \phi(x) - \frac{e}{kT_-} \phi(c_1) \quad , \quad x - c_1 = \lambda \xi \quad (44)$$

In these units the electron (25) and ion (24) pressures become

$$p_-(x) = \frac{kT_-}{e} \frac{j_-}{\langle |v_-| \rangle} P(-\eta^{1/2}(x)) \quad (45)$$

$$p_+(x) = \frac{kT_+}{e} \frac{j_+}{\langle |v_+| \rangle} P\left(-\left(\frac{T_-}{T_+}\right)^{1/2} \left(\eta(a_1) - \eta(x)\right)^{1/2}\right) \sim \quad (46)$$

$$-2\pi^{-1/2} \frac{kT_-}{e} \frac{j_+}{\langle |v_-| \rangle} \left(\frac{m_+}{m_-}\right)^{1/2} \left(\eta(a_1) - \eta(x)\right)^{1/2} \approx \text{const.} - \frac{kT_-}{e} \frac{j_+}{\langle |v_-| \rangle} \frac{\langle |v_-| \rangle}{v_+(c_1)} \eta(x)$$

In writing (46) only linear variations of the ion velocity (31) have been taken into account within the electron trap.

With $j_-/j_+ = \tau$ and $\langle |v_-| \rangle / v_+(c_1) \approx \sigma$ the pressure balance (41) reads

$$\frac{1}{2} \left(\frac{d\eta}{dx}\right)^2 = \tau P\left(-\eta^{1/2}\right) - \sigma \eta - \tau + C \quad (47)$$

The integration of this differential equation was performed on the Stanford IBM 7090 digital computer using an Adams Predictor-Corrector procedure⁴. Plots of pressure, electric field and distance versus potential obtained for $\tau = 0.01$ and three different velocity ratios $\sigma = 2, 1, 1/2$ are shown in Fig. 6. The constants of integration C have been adjusted such that the electric field at plasma potential $\phi(b_1)$ is the same in all three cases. The corresponding distances $c-c_1$ between cathode and accelerator grid are also listed in table I.

V. PLASMA-LIKE STATES $\sigma > 1$

To integrate the pressure balance within the region $x > c$ behind the ion motor we introduce again the scaling parameters

kT_-/e and the Debye length λ defined in (43). We shall, however, count normalized potential and distance from a different origin $x = c_2$:

$$\eta(\xi) = \frac{e}{kT_-} \phi(x) - \frac{e}{kT_-} \phi(c_2) \quad , \quad x - c_2 = \lambda \xi \quad (48)$$

Taking only linear variations of the ion velocity (31) into account we have from (24) and (26) in analogy with (45) and (46):

$$p_- = \frac{kT_-}{e} \frac{j_-}{\langle |v_-| \rangle} P(\eta^{1/2}) \quad (49)$$

$$p_+ = \text{const.} - \frac{kT_-}{e} \frac{j_+}{\langle |v_-| \rangle} \frac{\langle |v_-| \rangle}{v_+(c_2)} \eta \quad (50)$$

With $j_-/j_+ = 1$ and $\langle |v_-| \rangle / v_+(c_2) = \sigma$ the pressure balance (41) becomes

$$\begin{aligned} \frac{1}{2} \left(\frac{d\eta}{d\xi} \right)^2 &= P(\eta^{1/2}) - \sigma \eta - 1 + C \\ &= C + (1-\sigma)\eta - \frac{4}{3} \pi^{-1/2} \eta^{3/2} + \frac{1}{2} \eta^2 - \dots \end{aligned} \quad (51)$$

We have used the first few terms of the power series (A4) for P to demonstrate the essential difference between plasma-like and beam-like states, $\sigma < 1$ and $\sigma > 1$. Postponing the discussion of beam-like states to the next section we take for the present $\sigma > 1$. With our sign convention (13), $\text{sgn } \eta^{1/2}(\xi) = \text{sgn}(\xi)$,

we then find a pressure minimum in the region $c < x < c_2$. This situation is demonstrated in a plot of pressure versus potential for $\sigma = 2$, shown in Fig. 7(a). Due to (A3), this minimum occurs exactly at the plasma potential $\phi(b_2)$ as given by (38). The constant of integration used in (51) must be selected such that the electric field is real throughout the region $c < x < c_2$ as shown in Fig. 7(b).

$$C \geq C_0 = 1 + \sigma\eta - P(\eta^{1/2}) \quad , \quad \eta = \frac{e}{kT_-}\phi(b_2) - \frac{e}{kT_-}\phi(c_2) \quad (52)$$

Diagrams of potential versus distance obtained by numerical integration of (51) for two values of C are shown in Fig. 7(c). For $C > C_0$ the distance between the electron emitter at $x = c$ and the 'floating target' at $x = c_2$ is finite, as in a Laboratory experiment. The results of several integrations allow one to pick the appropriate constant C for any given distance of the target. As $C \rightarrow C_0$ one approaches the case of an infinitely distant target. Yet the floating target is not redundant in this case. It provides for instant recombination of electrons and ions, thus producing a potential drop (sheath) to turn the excess electrons back as shown in Fig. 2(b). Several arguments may be advanced to the existence of this state in free space:

1) The effect of volume recombination may provide a gradual potential drop along the plasma column thus causing excess electrons to be returned.

ii) A potential drop (sheath) is formed at the head of the advancing ion beam which causes excess electrons to be returned³.

To evaluate the first assumption 1) we use a simple model describing the effect of recombination. Assuming neutrality $n_- = n_+ = n(b_2)$ and common drift velocity $\langle v_- \rangle = v_+(b_2)$ for both species we have

$$\frac{d}{dx} n v_+ = -\alpha n^2, \quad n = n(b_2) \left(1 + \alpha \frac{n(b_2)}{v_+(b_2)} x \right)^{-1} \quad (53)$$

where α , the coefficient of recombination, is less than $2 \cdot 10^{-11} \text{ cm}^{-3} \text{ sec}^{-1}$.¹⁰ The scale on which recombinations take place is thus given by

$$x_r = \frac{v_+(b_2)}{\alpha n_+(b_2)} = \frac{e v_+^2}{\alpha j_+} \quad (54)$$

For typical ion motors this distance turns out to be in excess of 900 km as listed in table I. Thus it appears that the effect of volume recombination may indeed justify the omission of the floating target and also secure the validity of our d.c. solution out to considerable distances behind the space vehicle, provided it is stable.

To assess the validity of assumption 11) we have tried to solve for the d.c. state in a frame of reference moving with the ions. Electrons are allowed to escape from and return to the head of the ion beam, very much like in the case of an electron emitter placed in free space. A self-consistent d.c. state is found to exist in the moving frame. However, it is not possible to match this solution to the electron emitting grid within the ion motor, simply by applying a Galileo transformation. We conclude that the sheath at the head of the advancing plasma beam is necessarily of an oscillating nature. The question of stability will be discussed in Section VII.

VI. BEAM-LIKE STATES $\sigma < 1$

Proceeding with our discussion of equation (51) we find a pressure maximum to exist for $\sigma < 1$ in the region $x > c_2$ behind the potential minimum $\phi(c_2)$ as shown in Fig. 8(a). Again due to (A3), this maximum occurs at exactly the plasma potential $\phi(b_2)$ as given by (38). If no auxiliary 'grids' are to be used behind the electron emitter the constant of integration C in (51) is necessarily equal to 0. For $x > c_2$ the relation between electric field and potential is cyclical as shown in Fig. 8(b) and the potential becomes a periodic function of distance as seen in Fig. 8(c). All the excess electrons are returned before they reach

the potential minimum a finite distance downstream and the flow of electrons and ions becomes unidirectional thereafter as shown in Fig. 3(b). The floating target is thus redundant and this state may actually exist in free space, provided it is stable.

The potential diagram shown in Fig. 8(c) has been obtained by numerical integration of (51) for $\sigma = 1/2$, $C = 0$. However, by means of the excellent approximation $P_1(x)$ (eq. (17), Fig. 5) an analytic solution can be found in the periodic region

$$\frac{1}{2} \left(\frac{d\eta}{d\xi} \right)^2 \approx \frac{1 + 1/2(\pi\eta)^{1/2} + \eta}{1 + 1/2(\pi\eta)^{1/2}} - \sigma\eta - 1 \quad (55)$$

With $(\pi\eta)^{1/2}$ as auxiliary variable, a solution satisfying the boundary condition $\xi = 0$, $\eta = 0$ is obtained in the form

$$\begin{aligned} (\pi/2)^{1/2} \sigma^{3/2} \xi &= 2\sigma^{1/2}(1-\sigma)^{1/2} + \arcsin(1-2\sigma) \\ &\quad - \sigma^{1/2} \left(2-2\sigma-\sigma(\pi\eta)^{1/2} \right)^{1/2} \left(2+(\pi\eta)^{1/2} \right)^{1/2} - \arcsin(1-2\sigma(\pi\eta)^{1/2}) \end{aligned} \quad (56)$$

Values of potential obtained from (56) are compared in Fig. 8(c) with the results of numerical integrations of (51) using for P the rigorous expression (16). Note that (56) is good also for some negative values of ξ . A study of the inflection points and maxima of the potential diagram as given by (56) yields the following approximations:

1) Plasma potential at $x = b_2$

$$\eta = \frac{e}{kT_-} \phi(b_2) - \frac{e}{kT_-} \phi(c_2) \approx \frac{1}{4\pi\sigma^2} (1 - 4\sigma + (1 + 8\sigma)^{1/2})^2 \quad (57)$$

11) Maximum potential at $x = a_2$

$$\eta = \frac{e}{kT_-} \phi(a_2) - \frac{e}{kT_-} \phi(c_2) \approx \frac{4}{\pi\sigma^2} (1 - \sigma^2) \quad (58)$$

111) Period $c_3 - c_2$

$$\frac{c_3 - c_2}{\lambda} \pi^{1/2} \left(\frac{\sigma}{2}\right)^{3/2} \approx \frac{\pi}{2} + 2\sigma^{1/2} (1 - \sigma)^{1/2} + \arcsin(1 - 2\sigma) \quad (59)$$

Using the definition $\sigma \equiv \langle v_- \rangle / v_+(c_2)$ and Langmuir-Child's law (32) we have also

$$\frac{\lambda}{c_1 - a_1} = \frac{3}{2} \left(\frac{\pi m_-}{m_+}\right)^{1/2} \left(\frac{\phi(a_1) - \phi(c_2)}{\phi(a_1) - \phi(c_1)}\right)^{3/4} \sigma^{3/2} \quad (60)$$

Thus we obtain from (57), (58) and (59) in the limit of cold electrons $\sigma \rightarrow 0$

$$\frac{\phi(b_2) - \phi(c_2)}{\phi(a_1) - \phi(c_2)} = \frac{m_-}{m_+} \quad \text{or } v_-(b_2) = v_+(c_2) \quad (61)$$

$$\frac{\phi(a_2) - \phi(c_2)}{\phi(a_1) - \phi(c_2)} = 4 \frac{m_-}{m_+} \quad \text{or } v_-(a_2) = 2v_+(c_2) \quad (62)$$

$$\frac{c_3 - c_2}{c_1 - a_1} = 3\pi \left(\frac{2m_-}{\pi_+} \right)^{1/2} \left(\frac{\phi(a_1) - \phi(c_2)}{\phi(a_1) - \phi(c_1)} \right)^{3/4} \approx 3\pi \left(\frac{2m_-}{m_+} \right)^{1/2} \quad (63)$$

These formulae agree with results published previously on the problem of mixing cold electrons and ions^{1,2}.

To assess the effect of electron temperature, it is convenient to normalize plasma potential, maximum potential and period to their respective values for cold electrons. Thus rewriting (57), (58) and (59) we have

$$\frac{(\phi(b_2) - \phi(c_2))_{\text{hot}}}{(\phi(b_2) - \phi(c_2))_{\text{cold}}} \approx \frac{1}{4} (1 - 4\sigma + (1 + 8\sigma)^{1/2})^2 \quad (64)$$

$$\frac{(\phi(a_2) - \phi(c_2))_{\text{hot}}}{(\phi(a_2) - \phi(c_2))_{\text{cold}}} \approx (1 - \sigma)^2 \quad (65)$$

$$\frac{(c_3 - c_2)_{\text{hot}}}{(c_3 - c_2)_{\text{cold}}} \approx \frac{1}{2} + \frac{1}{\pi} \arcsin(1 - 2\sigma) + \frac{2\sigma^{1/2}}{\pi} (1 - \sigma)^{1/2} \quad (66)$$

These ratios are plotted in Fig. 10 and for $\langle |v_-| \rangle = v_+$ plasma potential, maximum potential and period are seen to vanish. In this borderline case the plasma becomes uniform in space $x > c_2$ as shown in Fig. 9(b). The variation of potential

versus distance for $x < c_2$ has been obtained by numerical integration of (51) for $\sigma = 1$, $C = 0$.

Before we conclude these sections on d.c. states, we add a few remarks on the thrust of the ion motor. It is evaluated by adding up the pressure on the accelerating and electron emitting grids. The pressure of the ions on the accelerator grid is given by

$$p(c_1-0) = \frac{1}{2} \epsilon_0 E^2(c_1-0) = mn_+(c_1)v_+^2(c_1) = \frac{m_+}{e} j_+ v_+(c_1) \quad (67)$$

with numerical values listed in table I. The contribution due to the neutralizer is found from the pressure balance (42). In normalized units we have

$$\frac{-p(c_1+0)+p(c-0)-p(c+0)}{p(c_1-0)} = \frac{\pi}{4} \frac{m_-}{m_+} \sigma \left(-\left(\frac{d\eta}{d\xi}\right)^2_{x=c_1+0} + \left(\frac{d\eta}{d\xi}\right)^2_{x=c-0} - \left(\frac{d\eta}{d\xi}\right)^2_{x=c+0} \right) \quad (68)$$

For small emitter bias this contribution was found to be negligibly small.

VII. STABILITY ANALYSIS

Within a uniform plasma of infinite extension a small signal analysis based on longitudinal perturbations $\propto \exp(i\omega t - ikx)$ yields the dispersion relation

$$k^2 = \int \frac{\omega_{p+}^2 F^+(v) + \omega_{p-}^2 F^-(v)}{\left(v - \frac{\omega}{k}\right)^2} dv \quad (69)$$

where $\omega_{p\pm}$ are the normalized plasma frequencies and $F^{\pm}(v)$ the normalized distribution functions of the electrons and ions respectively¹¹. This dispersion relation is well defined in the limit $\text{Im}\omega \rightarrow 0^-$, which arises when one employs Laplace analysis in time.

We have seen that in our case the d.c. analysis predicts an infinite region of almost uniform potential within the plasma emerging from the ion motor. The deviations from plasma potential were found to be very much smaller than kT_-/e for practical values of the parameter σ . Application of the dispersion relation (69) is therefore justified using

$$\omega_{p\pm}^2 = \frac{e}{\epsilon_0 m_{\pm}} q_{\pm}(b_2) = \frac{e}{\epsilon_0 m_{\pm}} \frac{j_{\pm}}{\langle |v_{\pm}| \rangle} \sigma \quad (70)$$

$$F^{\pm}(v) \equiv f^{\pm}(b_2, v) / \int f^{\pm}(b_2, v) dv = e f^{\pm}(b_2, v) / q_{\pm}(b_2) \quad (71)$$

with 10, 21; 12, 23; 30, 31, 38 we have

$$F^+(v) = \frac{m_+}{kT_+} v_+(b_2) \exp\left(\frac{m_+}{2kT_+} v_+^2(b_2) - \frac{m_+}{2kT_+} v^2\right) H(v - v_+(b_2)) \quad (72)$$

$$F^-(v) = \frac{m_-}{kT_-} v_+(b_2) \exp\left(\eta(b_2) - \frac{1}{\pi} \frac{v^2}{\langle |v_-| \rangle^2}\right) H\left(\frac{v}{\langle |v_-| \rangle} - \pi^{1/2} \pi^{1/2}(b_2)\right) \quad (73)$$

A plot of the weighted distribution function

$$\omega_{p_-}^2 F(v) \equiv \omega_{p_-}^2 F^-(v) + \omega_{p_+}^2 F^+(v) \quad (74)$$

in the numerator of (69) is shown in Fig. 11 for $\sigma = 2$ and $\sigma = 1$. Due to a criterion by Penrose¹² and Buneman¹³ we suspect that this doubly peaked distribution function is unstable. However, direct application of this simple criterion fails in our case due to the discontinuities in the distribution function $F(v)$. To explore the existence of growing modes we apply Cauchy's theorem to (69) on a contour enclosing the lower frequency half plane $\text{Im}\omega < 0$. In this process we make use of the fact that $m_+ v_+^2 / 2kT_+ \gg 1$ so that for all practical purposes $F^+(v)$ may be approximated by a Dirac δ -function:

$$F^+(v) \approx \frac{m_+}{kT_+} v_+(b_2) \exp\left(\frac{m_+}{kT_+} v_+(b_2)(v_+(b_2) - v)\right) H(v - v_+(b_2)) \sim \delta(v - v_+(b_2)) \quad (75)$$

With the ions thus behaving like a monoenergetic stream of particles the dispersion relation becomes:

$$K^2 = 2\pi^{-3/2} \sigma^{-1} \int_{\eta^{1/2}(b_2)}^{\infty} \exp(\eta(b_2) - t^2) \left(t - \frac{\Omega}{K} \pi^{-1/2}\right)^{-2} dt + \frac{m_-}{m_+} \left(\frac{1}{\sigma} - \frac{\Omega}{K}\right)^{-2} \quad (76)$$

where

$$K \equiv k \langle |v_-| \rangle / \omega_{p_-}, \quad \Omega \equiv \omega / \omega_{p_-}, \quad \text{Im} \Omega < 0 \quad (77)$$

This integral cannot be evaluated in closed form. However, the singularities arising for $\text{Im} \Omega \rightarrow 0^-$ can be extracted and the remaining integral computed (Appendix B). A plot of the right hand side of the dispersion relation (76) in the complex K^2 -plane is shown in Fig. 12 for the limit of real frequencies $\text{Im} \Omega \rightarrow 0^-$ and a velocity ratio $\sigma = 2$. The running parameter in this graph is the wave velocity Ω/K , with K real. Note that for any positive wavenumber K the point K^2 is encircled once as Ω varies from $-\infty$ to $+\infty$ and then along a large semicircle in the lower frequency half plane. Thus, for any positive wavenumber K , the dispersion relation (76), has precisely one solution Ω with $\text{Im} \Omega < 0$. Similar diagrams are obtained for other values of σ . We thus conclude that the one-dimensional d.c. states derived in the previous sections are all unstable.

A crude approximation estimates the wavenumber for which maximum growth occurs as $k \approx \omega_{p_-} / v_+^{11}$. The linear scale of these instabilities is thus of the order of several Debye lengths:

$$x_f = 2\pi v_+ / \omega_{p_-} = 2\pi \langle |v_-| \rangle / (\sigma \omega_{p_-}) \quad (78)$$

Within a few times that distance behind the ion motor these oscillations will have reached the nonlinear limit. Since $x_f \ll x_r$, the effect of recombinations discussed in section V is completely irrelevant. The question arises whether the r.f. amplitude developing behind the space vehicle remains small compared with the accelerating potential of the ions or becomes comparable to it. Accordingly the ion motor would work continuously or in discrete puffs. One dimensional computer simulations of the processes involved in the nonlinear motion of electrons and ions predict continuous operation with velocity randomization and rather strong potential fluctuations at electron plasma frequency^{14,15}.

Instabilities have been observed recently in experiments with cesium ion beams, using an electron emitting wire as the neutralizing element and a floating collector¹⁶. Oscillations near electron plasma frequency set in whenever the neutralizer is removed to the edge of the beam in which case the electrons are injected with higher than thermal energy. With the neutralizer located at the center of the beam, the plasma was found in an apparently stable state. The latter observation is in contradiction with our prediction and the discrepancy may arise from the finite lateral size of the experimental plasma not taken into account in the theory. We note, however, that

fluctuations over a broad band of frequencies may still be present in this experiment. These fluctuations are associated with an increase in electron temperature^{17,18} and should be detectable either by a probe or by noise measurements. Future experimental work should be supplemented by such measurements in order that the proper conclusions can be drawn. Progress on the theoretical side is expected from computer simulations of the nonlinear mixing process, the finite size of the plasma being an integral part of the program.

VIII. SUMMARY OF CONCLUSIONS

The character of d.c. states arising in the process of neutralizing ions emerging at equal rates with electrons from the nozzle of an ion motor depends critically upon σ , the mean thermal speed of the emitted electrons, as compared to the escape velocity of the ions.

For small electron temperatures $\sigma < 1$, excess electrons are returned to the ion motor from a potential minimum a short distance behind the space vehicle. The potential distribution becomes periodic in space thereafter.

For large electron temperatures $\sigma > 1$, plasma-like potential distributions are obtained behind the ion motor.

A floating target is required in this case to reflect the excess electrons back to their source. Recombinations occurring a long distance behind the space vehicle may lift this requirement.

Arguments of whether or not these d.c. states do exist in outer space find a unique answer when it is learned that all are unstable with respect to small perturbations. A large signal theory describing the nonlinear mixing process of electrons and ions within a plasma beam of essentially finite lateral dimensions is required to interpret and project experimental results into actual space environment.

Acknowledgements

The author wishes to thank Professor O. Buneman for his helpful criticism in the preparation of this paper and Mr. T.C. Jackson and Mrs. M.F. O'Neal for programming the numerical work on the Stanford IBM 7090 Computer. This work was supported by the National Aeronautics and Space Administration under grant NsG-299-63.

APPENDIX A: SERIES REPRESENTATION OF CHARGE AND PRESSURE FUNCTIONS

The charge and pressure functions are defined by the following integrals:

$$Q(x) = 2\pi^{-1/2} \int_x^\infty e^{x^2-t^2} dt = e^{x^2} \operatorname{erfc}(x) \quad (A1)$$

$$P(x) = 4\pi^{-1/2} \int_x^\infty t^2 e^{x^2-t^2} dt = 2\pi^{-1/2} x + Q(x) \quad (A2)$$

$$\frac{dP}{dx} = 2xQ \quad (A3)$$

Representations in terms of power series and asymptotic series are obtained immediately by writing the error function in terms of confluent hypergeometrical functions of the first (Φ) and second kind (Ψ), respectively¹⁹.

$$\begin{aligned} Q(x) &= e^{x^2} \operatorname{erfc}(x) \\ &= e^{x^2} - 2\pi^{-1/2} x \Phi(1, 3/2, x^2) = e^{x^2} - 4\pi^{-1/2} x \sum_{n=0}^{\infty} \frac{(n+1)!}{(2n+2)!} (2x)^{2n} \end{aligned} \quad (A4)$$

$$= \pi^{-1/2} \Psi(1/2, 1/2, x^2) \sim 2H(-x)e^{x^2} + \frac{\pi^{-1/2}}{x} \sum_{n=0}^N (-1)^n \frac{(2n)!}{n!} (2x)^{-2n} \quad (A5)$$

where $H(x)$ is the unit step function.

For numerical purposes Fried's Tables of the Hilbert Transform of the Gaussian may also be used noting that $Q(x) = -i \pi^{-1/2} Z(ix)$.²⁰

The simple approximation $P_1(x)$ given by formula (19) in the text is suggested by the fact that every confluent hypergeometrical function can be expanded into continued fractions. The actual procedure used to obtain $P_1(x)$ is to match the expression $P_1(x) = (a + bx + cx^2)/(d + ex)$ with the power series (A4) for small x and with the asymptotic series (A5) for large x . The error of this approximation is within 3 percent in the range $-0.6 < x < +\infty$.

APPENDIX B: EVALUATION OF DISPERSION INTEGRAL

The integral (76) to be calculated is of the form

$$\int_y^{\infty} \frac{f(x)}{(x-z)^2} dx, \quad \text{Im}x = \text{Im}y = 0, \quad \text{Im}z < 0, \quad f(\pm \infty) = 0 \quad (\text{B1})$$

where $f(x)$ is continuous for real x .

A partial integration yields

$$\begin{aligned} \int_y^{\infty} \frac{f(x)}{(x-z)^2} dx &= \frac{f(y)}{y-z} + \int_y^{\infty} \frac{f'(x)}{x-z} dx = \frac{f(y)}{y-z} \\ &+ \int_y^{\infty} \left(\frac{f'(z)}{x-z} - \frac{xf'(z)}{1+x^2} \right) dx + \int_y^{\infty} \left(\frac{f'(x)-f'(z)}{x-z} + \frac{xf'(z)}{1+x^2} \right) dx \end{aligned} \quad (\text{B2})$$

The first integral is singular but can be evaluated

$$\int_y^{\infty} \left(\frac{f'(z)}{x-z} - \frac{xf'(z)}{1+x^2} \right) dx = -f'(z) \#n \frac{y-z}{(1+y^2)^{1/2}} \quad (\text{B3})$$

where $\#n$ stands for the principal value of the logarithm. The last integral is regular everywhere including the points $x = y, z, \infty$. A more convenient form for computation is obtained with the substitutions

$$x = \text{tg } \xi, \quad y = \text{tg } \eta, \quad z = \text{tg } \zeta \quad (\text{B4})$$

$$\int_y^{\infty} \left(\frac{f'(x)-f'(z)}{x-z} + \frac{xf'(x)}{1+x^2} \right) dx = \int_{\eta}^{\infty} \left(\frac{f'(\text{tg } \xi)-f'(\text{tg } \zeta)}{\text{tg } (\xi-\zeta)} + f'(\text{tg } \xi) \text{tg } \xi \right) d\xi \quad (\text{B5})$$

With

$$J(\eta, \xi) \equiv \int_{\eta}^{\pi/2} \frac{f'(\operatorname{tg} \xi) - f'(\operatorname{tg} \eta)}{\operatorname{tg}(\xi - \eta)} d\xi \quad (\text{B6})$$

we have

$$\begin{aligned} \int_y^{\infty} \frac{f(x)}{(x-z)^2} dx &= \frac{f(y)}{y-z} - f'(z) \ln \frac{y-z}{(1+y^2)^{1/2}} \\ &+ J(\operatorname{arctg} y, \operatorname{arctg} z) - J(\operatorname{arctg} y, \pi/2) \end{aligned} \quad (\text{B7})$$

and in the limit $\operatorname{Im} z \rightarrow 0^-$

$$\begin{aligned} \int_y^{\infty} \frac{f(x)}{(x-z)^2} dx &= \frac{f(y)}{y-z} - f'(z) \ln \left| \frac{y-z}{(1+y^2)^{1/2}} \right| - i\pi f'(z) H(z-y) \\ &+ J(\operatorname{arctg} y, \operatorname{arctg} z) - J(\operatorname{arctg} y, \pi/2) \end{aligned} \quad (\text{B8})$$

where $H(x)$ is the unit step function. This formula was applied to evaluate (76) on the Stanford IBM 7090 digital computer by using a simple Simpson procedure for $J(\eta, \xi)$.

References

1. The staff of the Ramo-Woolridge Research Laboratory, "Electrostatic Propulsion," Proc. Inst. Radio Engrs., 48, 477 (1960).
2. V.P. Ignatenko, A.S. Myasinkov, "Neutralization of ion space charge by electrons," Radio Engineering and Electronic Physics (USSR) 6, 1868 (1961).
3. Harold Mirels, "On ion rocket neutralization," Symposium of the American Rocket Soc., Monterey, Calif., Nov. 3-4, 1960.
4. R. Cornog, "The optimum velocity of propellant ejection," Vistas in Astronautics, 1, 172 (1958).
5. J.M. Sellen, Jr. and H. Shelton, "Transient and steady state behavior in Cesium ion beams," Symposium of the American Rocket Soc., Monterey, Calif., Nov. 3-4, 1960.
6. M.J. Lighthill, Fourier Analysis and Generalized Functions, (Cambridge University Press, London, 1959), p. 29.
7. I.B. Bernstein, J.M. Greene and M.D. Kruskal, "Exact nonlinear plasma oscillations," Phys. Rev., 198, 546 (1957).
8. J.R. Pierce, Theory and Design of Electron Beams (D. Van Nostrand Company, Inc., New York, 1954).
9. F.B. Hildebrand, Introduction to Numerical Analysis (McGraw-Hill Book Company, Inc., New York, 1956) Chapter 6.
10. R.C. Knechtli and J.Y. Wada, "Quiescent Cesium plasma in steady state," Proc. of the Fifth International Conference on Ionization Phenomena in Gases, Munich, Aug. 28-Sept. 1, 1961, (North Holland Publishing Company, Amsterdam, 1962), p. 786.
11. O. Buneman, "Dissipation of currents in ionized media," Phys. Rev., 115, 303 (1959).
12. O. Penrose, "Electrostatic instabilities of a uniform non-Maxwellian plasma," Phys. Fluids, 3, 258 (1960).

13. O. Buneman, "Maintenance of equilibrium by instabilities," International Plasma Physics Institute, August 31-Sept. 5, Seattle, 1959 and J. Nuclear Energy, Part C Plasma Physics, 2, 119 (1961).
14. O. Buneman and G. Kooyers, "Computer simulation of the electron mixing process in ion propulsion," AIAA Electric Propulsion Conference, Colorado Springs, March 11-13, 1963.
15. D.A. Dunn and I.T. Ho, "Longitudinal instabilities in an electrostatic propulsion beam with injected current neutrality," AIAA Electric Propulsion Conference, Colorado Springs, March 11-13, 1963.
16. W. Bernstein and J.M. Sellen, Jr., "Oscillations in Synthetic Plasma Beams," Phys. Fluids 6, 1032 (1963).
17. O. Buneman, "Dissipation of currents in ionized media," Phys. Rev. 115, 503 (1959).
18. J.W. Dawson, "Nonlinear effects in electron plasmas," Phys. Rev. 113, pp. 383 (1959).
19. A. Erdelyi, W. Magnus, F. Oberhettinger and F.G. Tricomi, Higher transcendental functions (McGraw-Hill Book Company, Inc., New York, 1953), vol. I, Chap. 6.
20. Burton D. Fried and Samuel D. Conte, The Plasma Dispersion Function (Academic Press, New York, 1961), p. 3.

Table I Data for Three Ion Motors

A_1 : $\sigma = 2$ floating collector at $c_2 - c = 190.4 \lambda$

A_2 : $\sigma = 2$ floating collector at $c_2 - c = \infty$

B: $\sigma = 1$ no collector required

C: $\sigma = 1/2$ no collector required

* values obtained by numerical integration of equ. X

+ approximate values may be obtained from equ. X

Quantity	Symbol	Unit	A ₁	A ₂	Case	B	C	Formula
Compare Figure	#	/	2,6,7	2,6,7		6,9	3,6,8	
Anode Temperature	T ₊	°K		1350				
Cathode Temperature	T ₋	°K		2350				
Electron Current Temp. Ltd.	J _{s-}	mAcm ⁻²		50				Richardson
Electron Current Downstream	J ₋	mAcm ⁻²		5				33
Electron Current Upstream	J _{-j}	μAcm ⁻²		50				34
Ion Current (Caesium)	J ₊	mAcm ⁻²		5				32
Trapping Ratio	$\tau = J/J_+$	/		0.01				34
Mean Thermal Electron Speed	$\langle v_- \rangle$	km sec ⁻¹		150				28
Ion Escape Velocity	v _{+(c₂)}	km sec ⁻¹	75			150	300	31
Velocity Ratio	$\sigma = \langle v_- \rangle / v_+$		2			1	0.5	38
Thermal Electron Energy	kT ₋ /e	V	0.2			0.2	0.2	/
Acceleration Voltage	$\phi(a_1) - \phi(c_1)$	kV	3.9			15.6	62.4	32
Plasma Pot. in Electron Trap	$\phi(b_1) - \phi(c_1)$	kT ₋ /e	4.61			3.91	3.22	35
Emitter Bias	$\phi(c_-) - \phi(c_1)$	kT ₋ /e	6.91			6.91	6.91	36
Space or Floating Potential	$\phi(c_2) - \phi(c_1)$	kT ₋ /e	4.61			4.61	4.61	34
Plasma Potential in Space	$\phi(b_2) - \phi(c_2)$	kT ₋ /e	0.265			0	0.591	38,57 ⁺
Maxim. Potential in Space	$\phi(a_2) - \phi(c_2)$	kT ₋ /e	/			0	1.540	51*,58 ⁺
Electron Plasma Frequency	f _{p-}	mcy	579			410	290	70
Ion Plasma Frequency	f _{p+}	kcy	1172			829	586	70
Thrust	p	kg m ⁻²	0.53			1.06	2.12	67
Debye Length	λ	μ	73			73	73	43
Wavelength of Maximum Growth	x _f	λ	1.77			5.01	14.17	78
Recombination Distance	x _r	km	901			3605	14420	54
Distance Accel. Grid-Anode	c ₁ -a ₁	mm	4.80			13.57	32.38	32
Plasma -Accel. Grid	b ₁ -c ₁	λ	45.20			63.28	88.42	47*
Cathode -Accel. Grid	c -e ₁	λ	89.12			125.17	175.45	47*
Pot. min. -Cathode	c ₂ -c	λ	190.4	∞		3.29	1.78	51*
Plasma -Cathode	b ₂ -c	λ	95.7	∞		3.29	3.94	51*,56 ⁺
Plasma -Pot. min.	b ₂ -c ₂	λ	94.7	∞		0	2.16	51*,56 ⁺
Pot. max -Pot. min.	a ₂ -c ₂	λ	/	/		0	6.25	51*,59 ⁺
Periode Pot. min. -Pot. min.	c ₃ -c ₂	λ	/	/		0	12.50	51,59

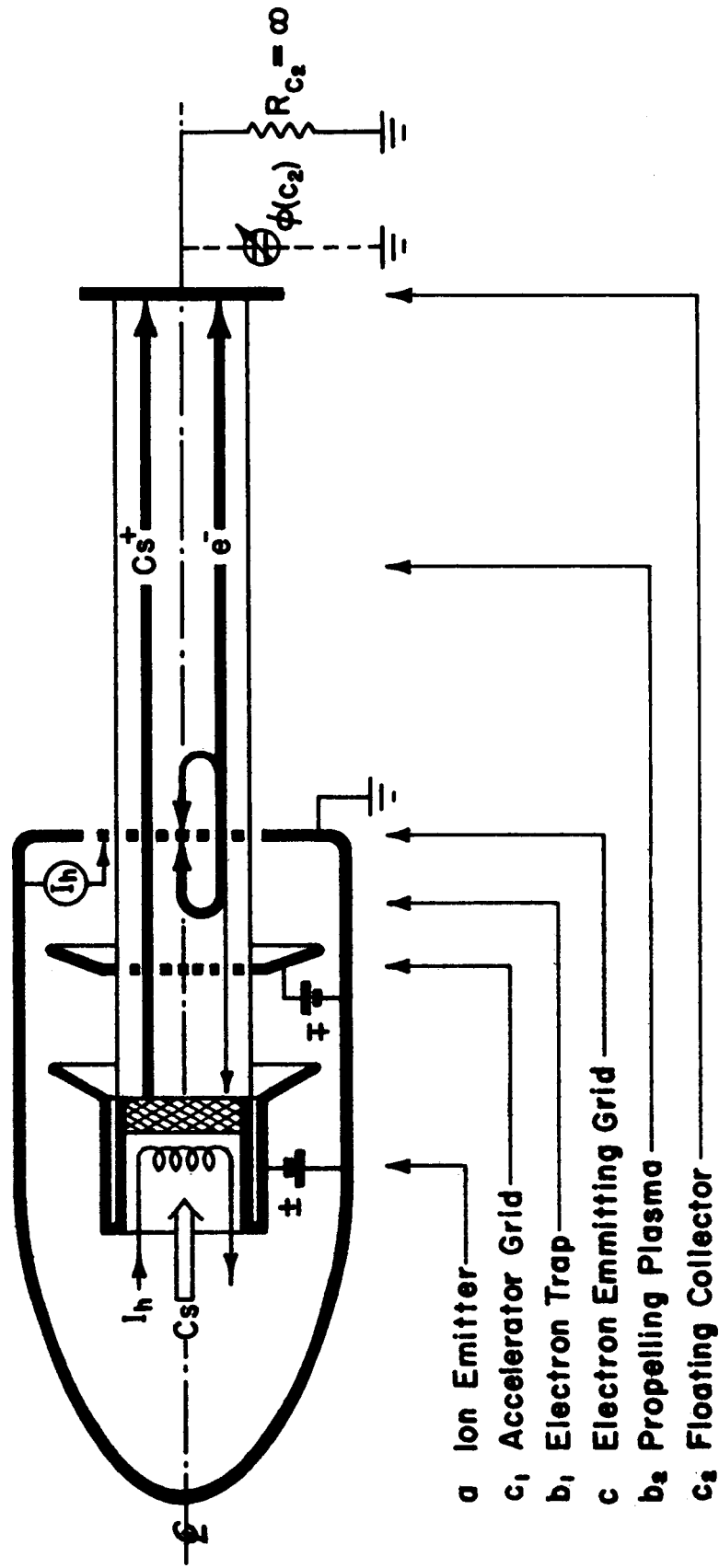


Fig. 1 Ion Motor (schematic)

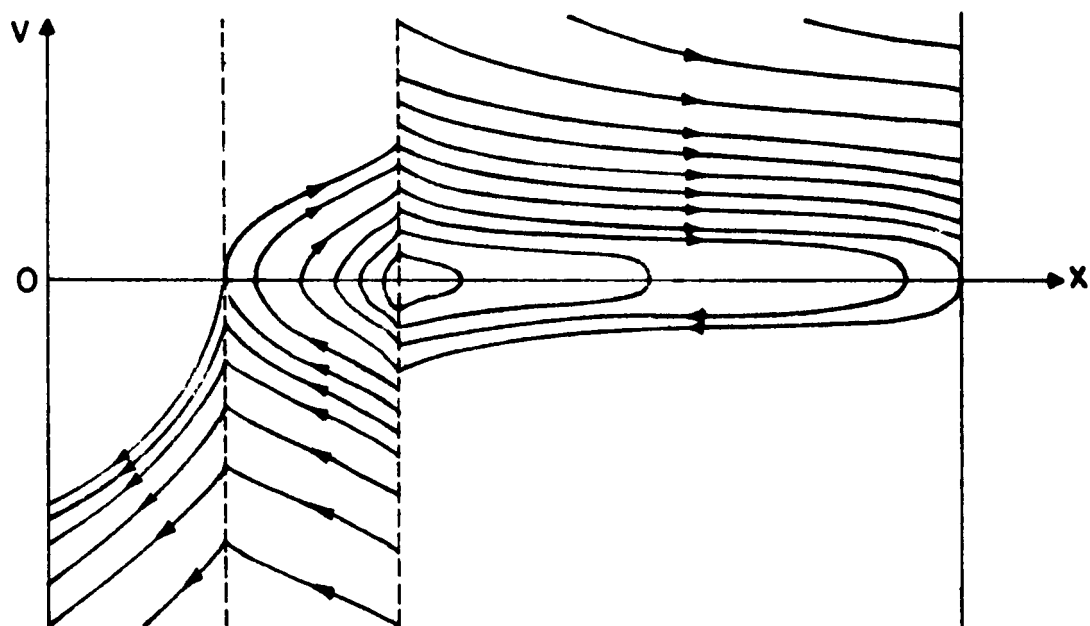
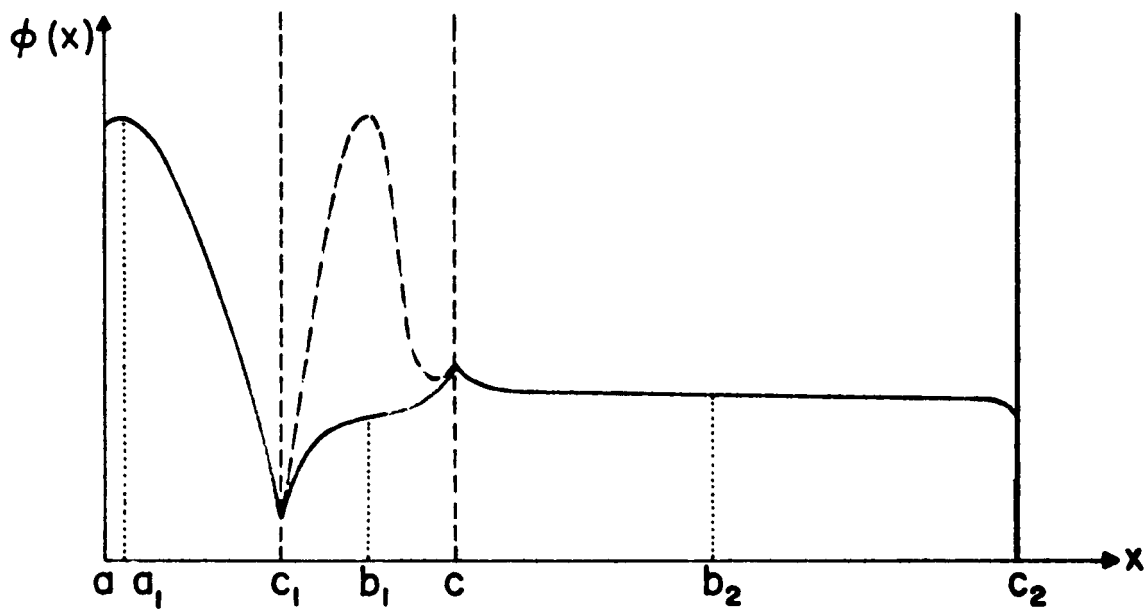


Fig. 2 (a) Potential Diagram of Ion Motor with Floating Collector and
(b) Corresponding Electron Orbits for $\sigma = \langle |v_-| \rangle / v_+(b_2) > 1$ (schematic)

----2(a) alternative potential for large cathode accelerator spacing $c-c_1$ and partial reflection of ions.

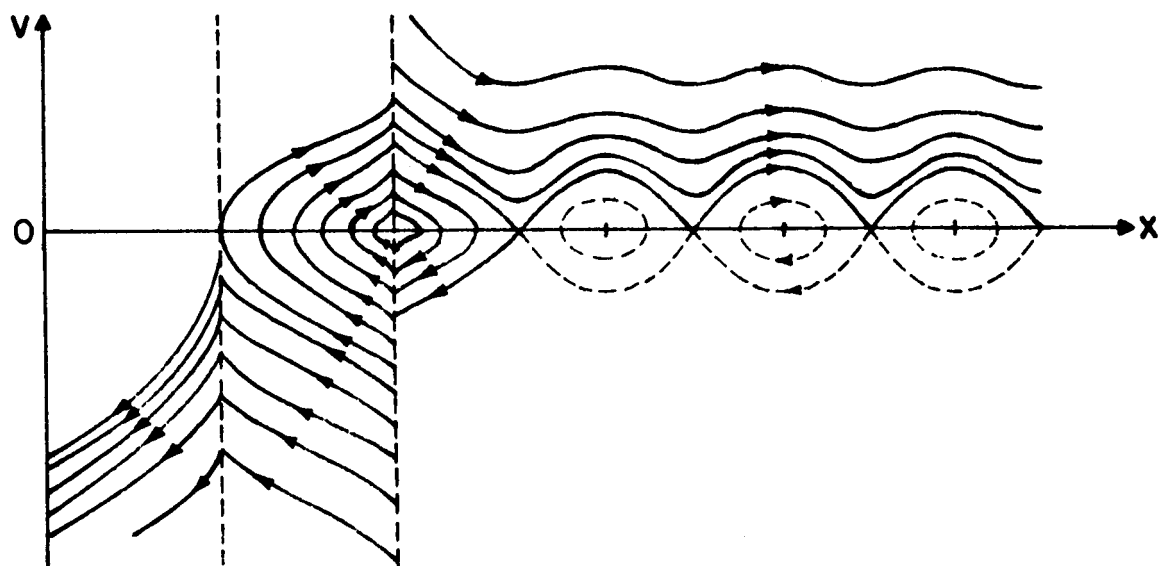
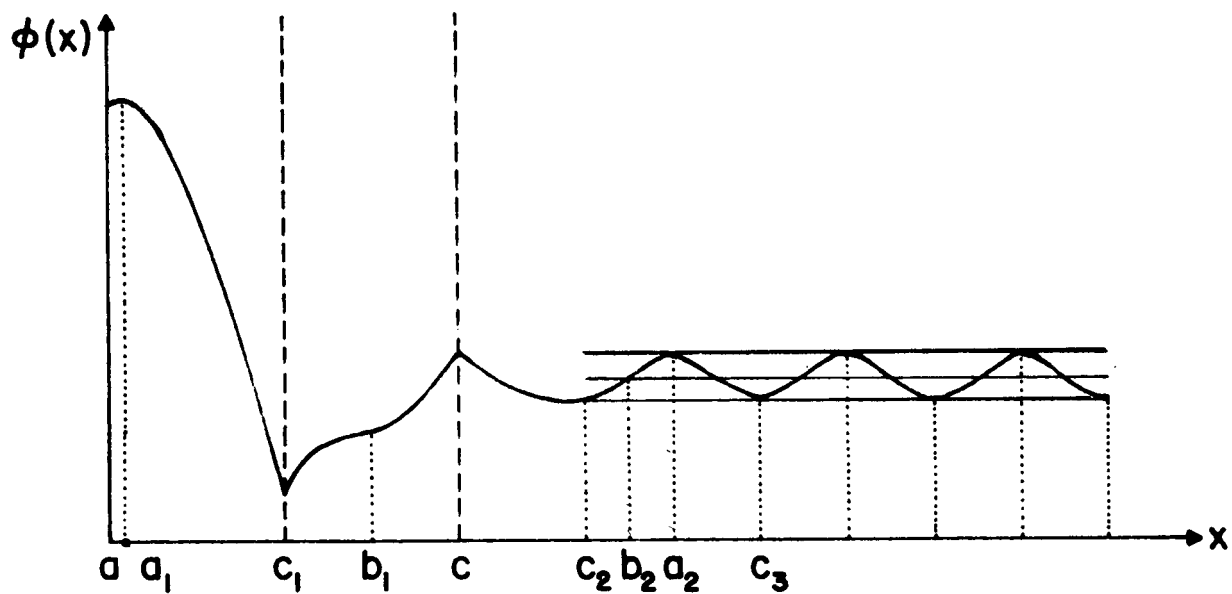


Fig. 3 (a) Potential Diagram of Ion Motor and
 (b) Corresponding Electron Orbits for
 $\sigma = \langle |v_-| \rangle / v_+(b_2) < 1$ (schematic)
 --- 3(b) orbits allowed for trapped electrons
 (traps are empty under d.c. conditions)

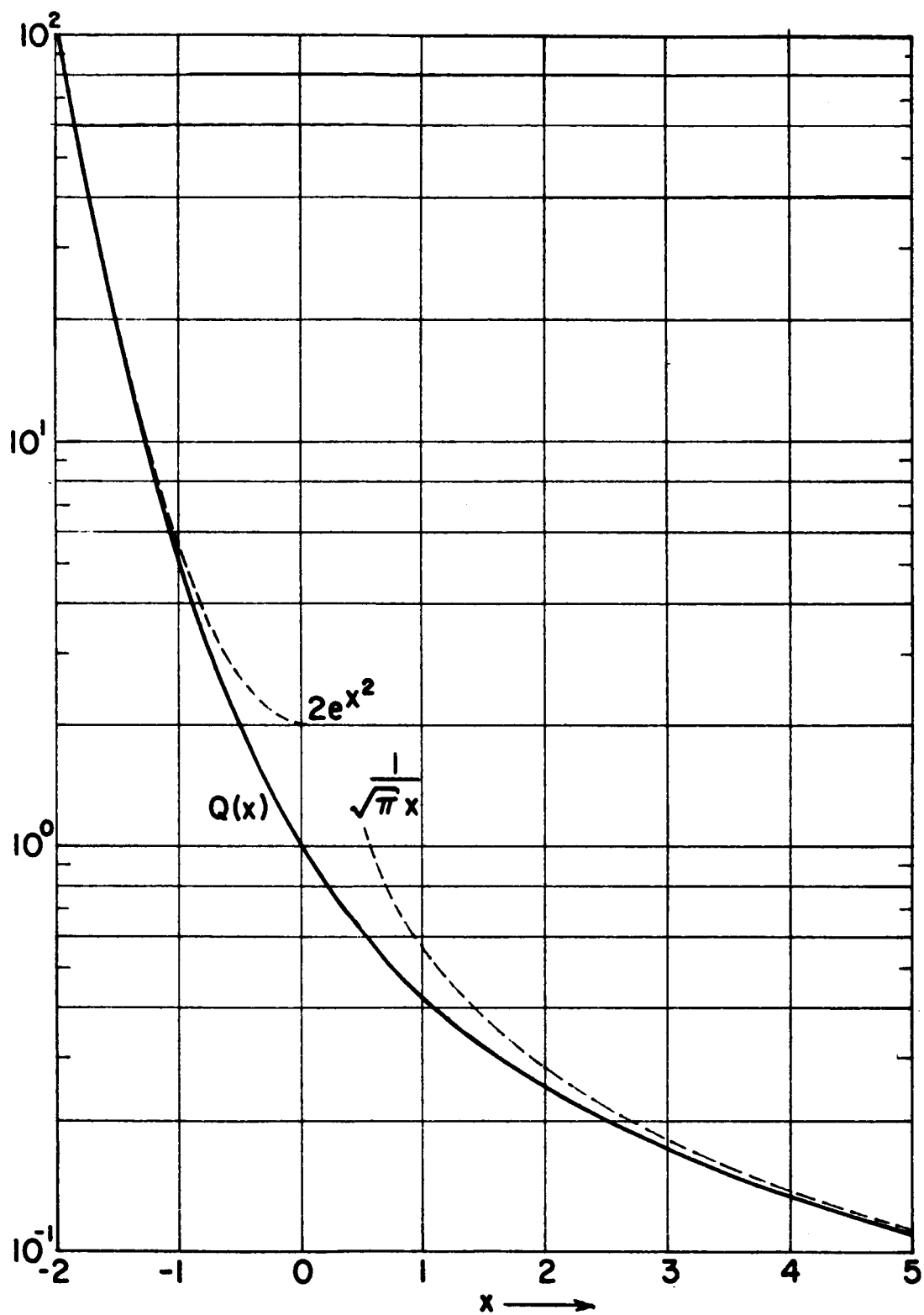


Fig. 4 Normalized Charge Density $Q(x)$ vs. Cutoff Velocity v_c of Gauss Distribution, $x = \pi^{-1/2} v_c / \langle |v_-| \rangle$.
 --- asymptotic laws: for $x \ll 0$ plasma-limit
 for $x \gg 0$ beam-limit

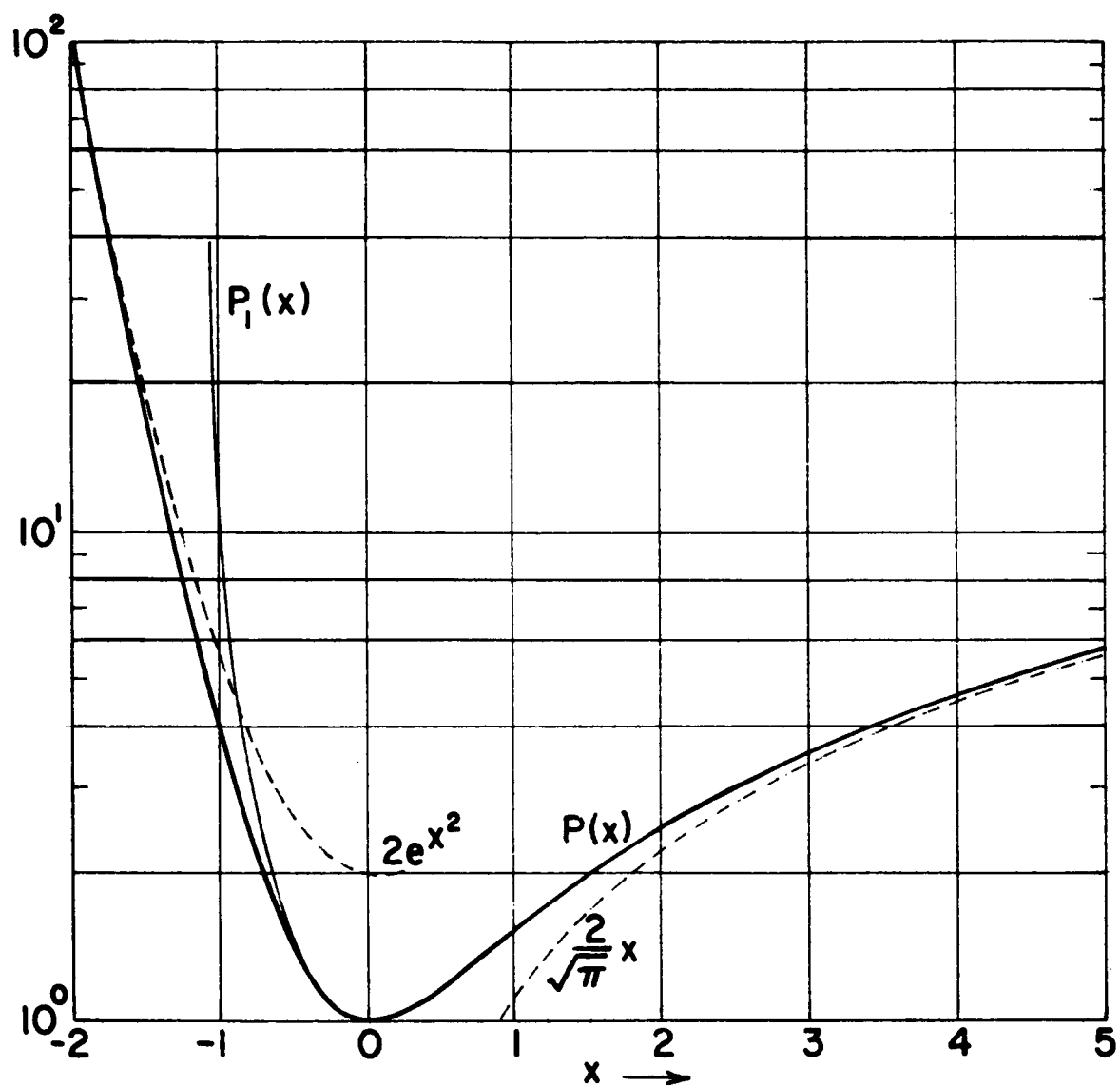


Fig. 5 Normalized Kinetic Pressure $P(x)$ vs. Cutoff Velocity v_c of Gauss Distribution, $x = \pi^{-1/2} v_c / \langle |v_-| \rangle$.

--- asymptotic laws: for $x \ll 0$ plasma-limit
for $x \gg 0$ beam-limit

— analytic approximation equ. (17)

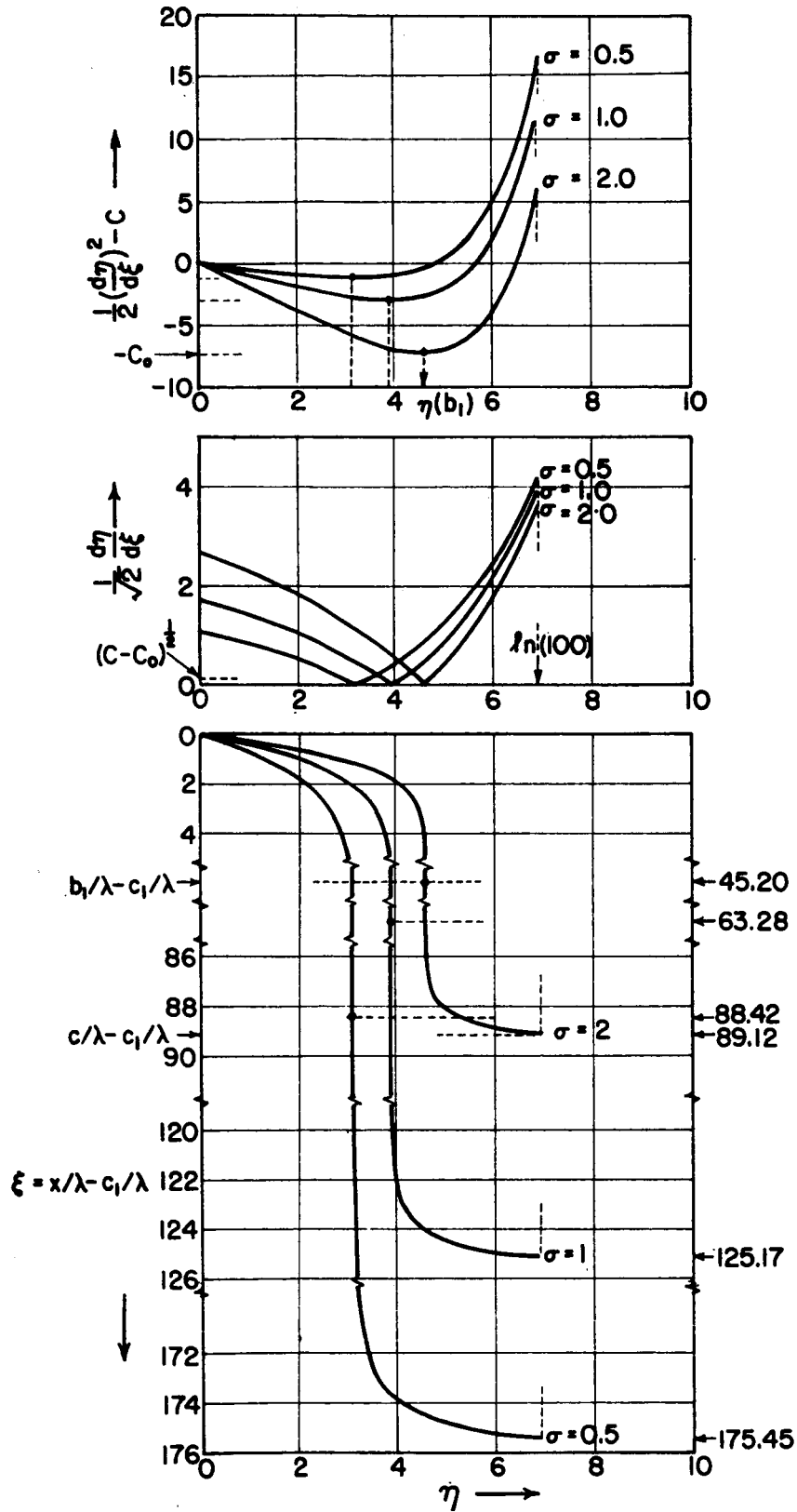


Fig. 6 (a) Pressure, (b) Electric Field and (c) Distance Within Electron Trap vs. Potential in Normalized Units

Trapping ratio $\tau = j_-/j_+ = 0.01$

Velocity ratio $\sigma = \langle |v_-| \rangle / v_+(c_1)$

Corresponding plasma potentials and pressure minima:

$$\sigma = 2 \quad \eta(b_1) = 4.60637 \quad C_0 = 7.24696$$

$$1 \quad 3.91460 \quad 2.94692$$

$$0.5 \quad 3.22444 \quad 1.14248$$

in all cases $C - C_0 = 10^{-53}$

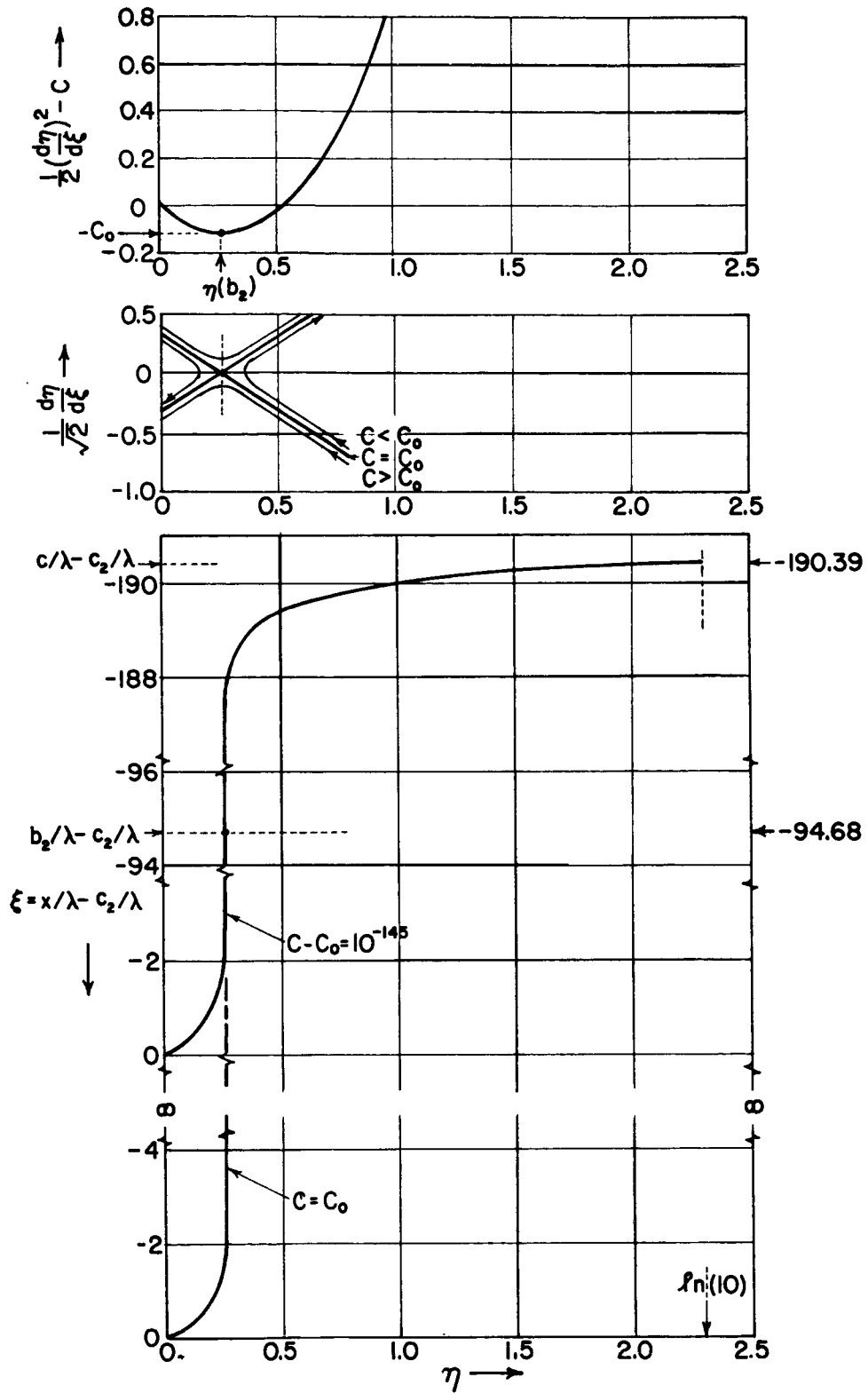


Fig. 7 (a) Pressure, (b) Electric Field and (c) Distance Within Propelling Plasma vs. Potential in Normalized Units
Trapping ratio $\tau = j_-/j_+ = 0.01$
Velocity ratio $\sigma = \langle |v_-| \rangle / v_+(c_2) = 2$
Corresponding plasma potential and pressure minimum:
 $\eta(b_1) = 0.265429$, $C_0 = 0.112197$.
for $C = C_0$ floating collector at $c_2 - c = \infty$

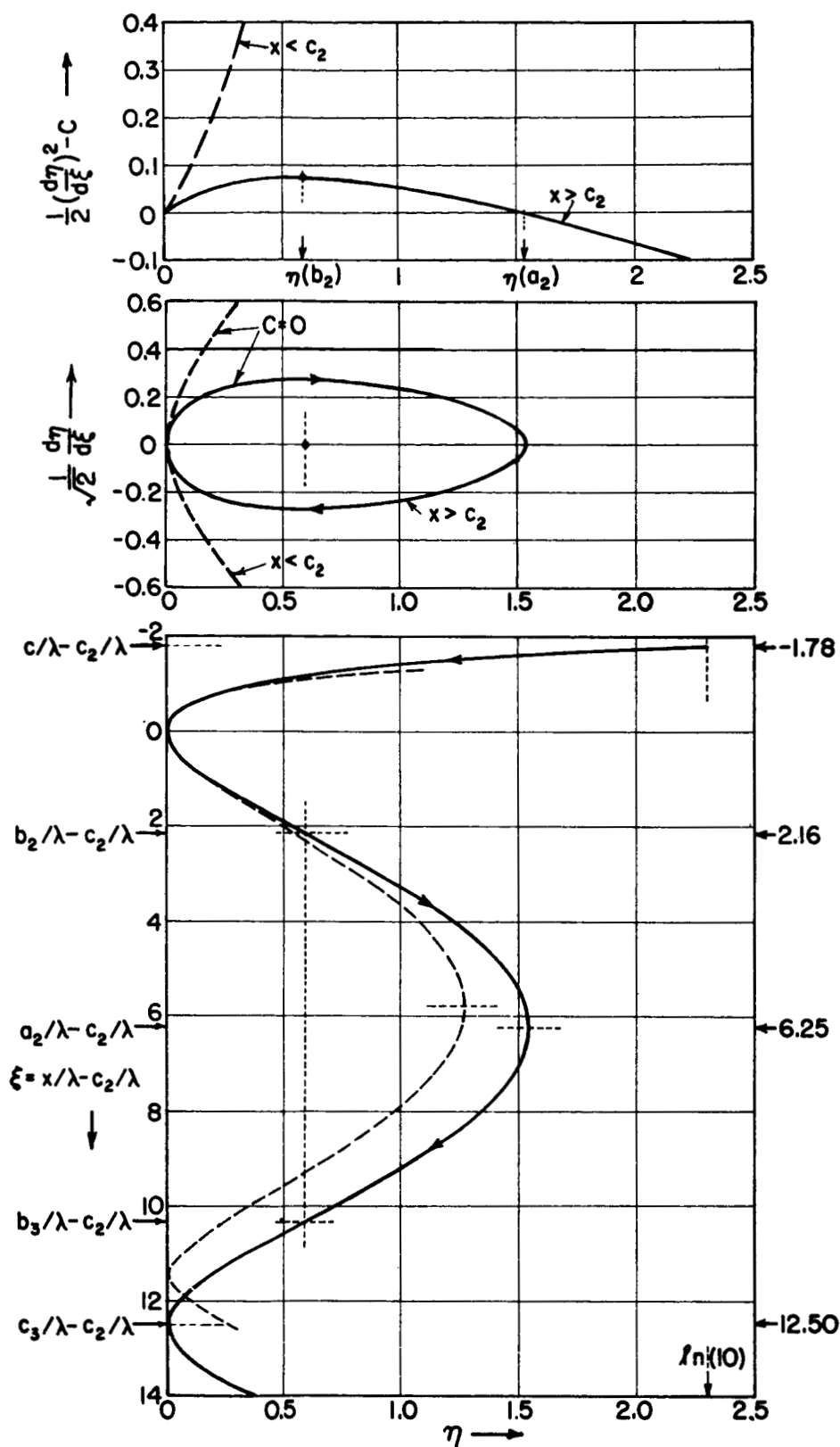


Fig. 8 (a) Pressure, (b) Electric Field and (c) Distance Within Propelling Plasma vs. Potential in Normalized Units
Trapping ratio $\tau = j_-/j_+ = 0.01$
Velocity ratio $\sigma = \langle |v_-| \rangle / v_+(c_2) = 0.5$
Corresponding plasma potential, maximum potential and period: $\eta(b_2) = 0.591483$, $\eta(a_2) = 1.53999$,
 $c_3 - c_2 = 12.5 \lambda$
----8(c) approximate solution equ. (56)

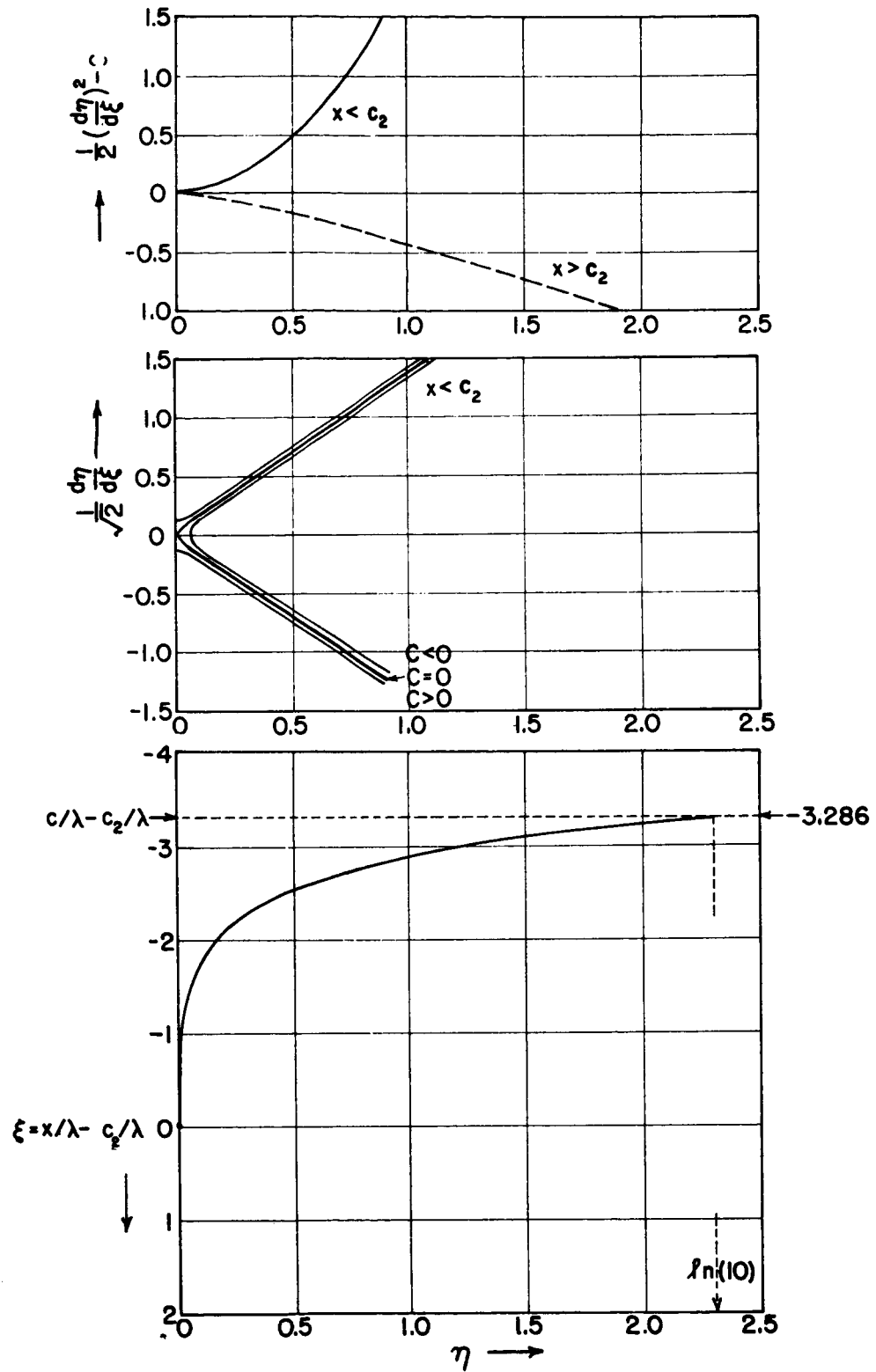


Fig. 9 (a) Pressure, (b) Electric Field and (c) Distance Within Propelling Plasma vs. Potential in Normalized Units
 Trapping ratio $\tau = j_-/j_+ = 0.01$
 Velocity ratio $\sigma = \langle |v_-| \rangle / v_+(c_2) = 1$
 Corresponding plasma potential, maximum potential and period: $\eta(b_2) = \eta(a_2) = c_3 - c_2 = 0$.

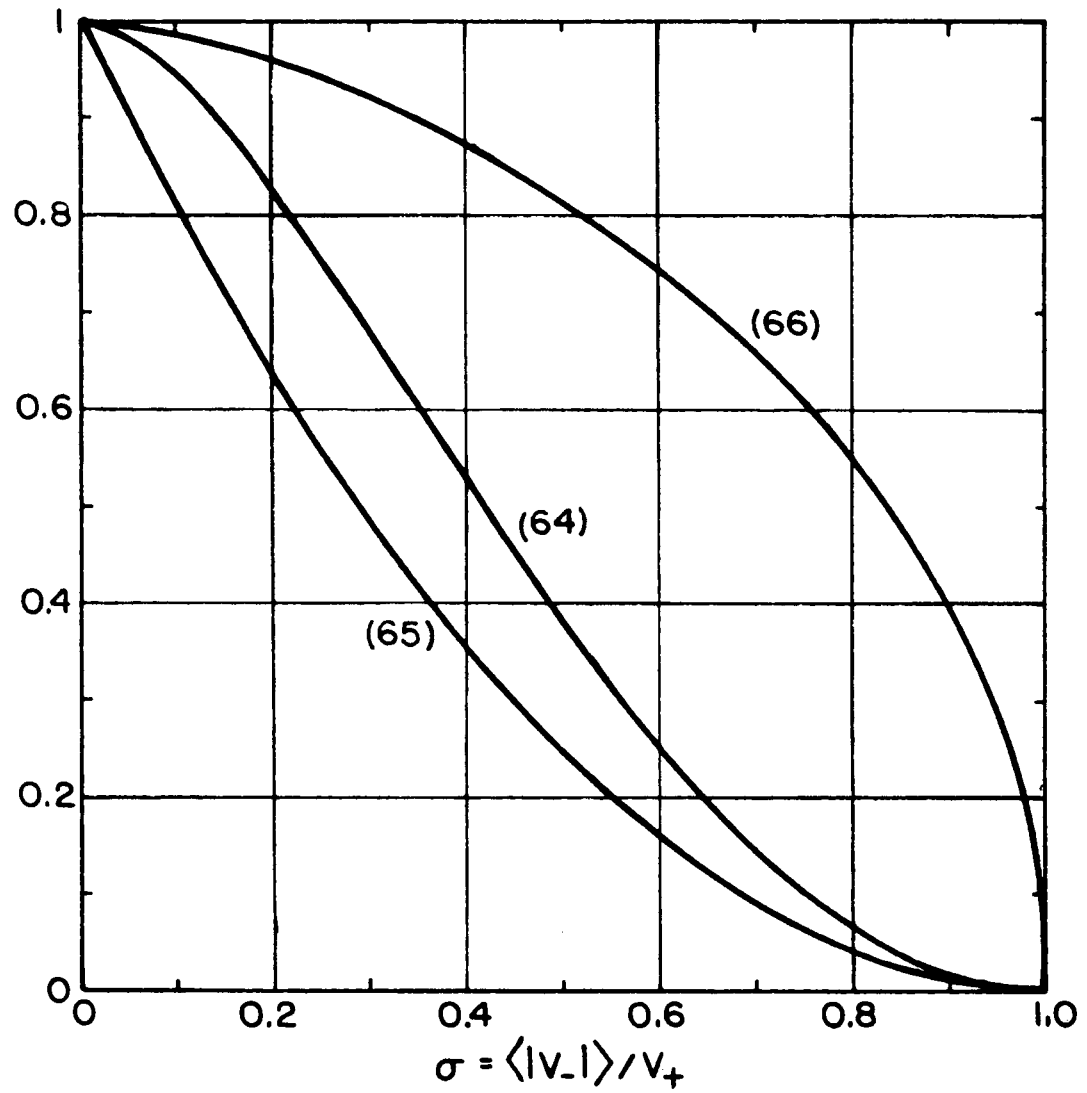


Fig. 10 Plasma Potential equ. (64), Maximum Potential equ. (65) and Period equ. (66) vs. Electron Temperature $\sigma = \langle |v_-| \rangle / v_+(c_2)$ in normalized units.

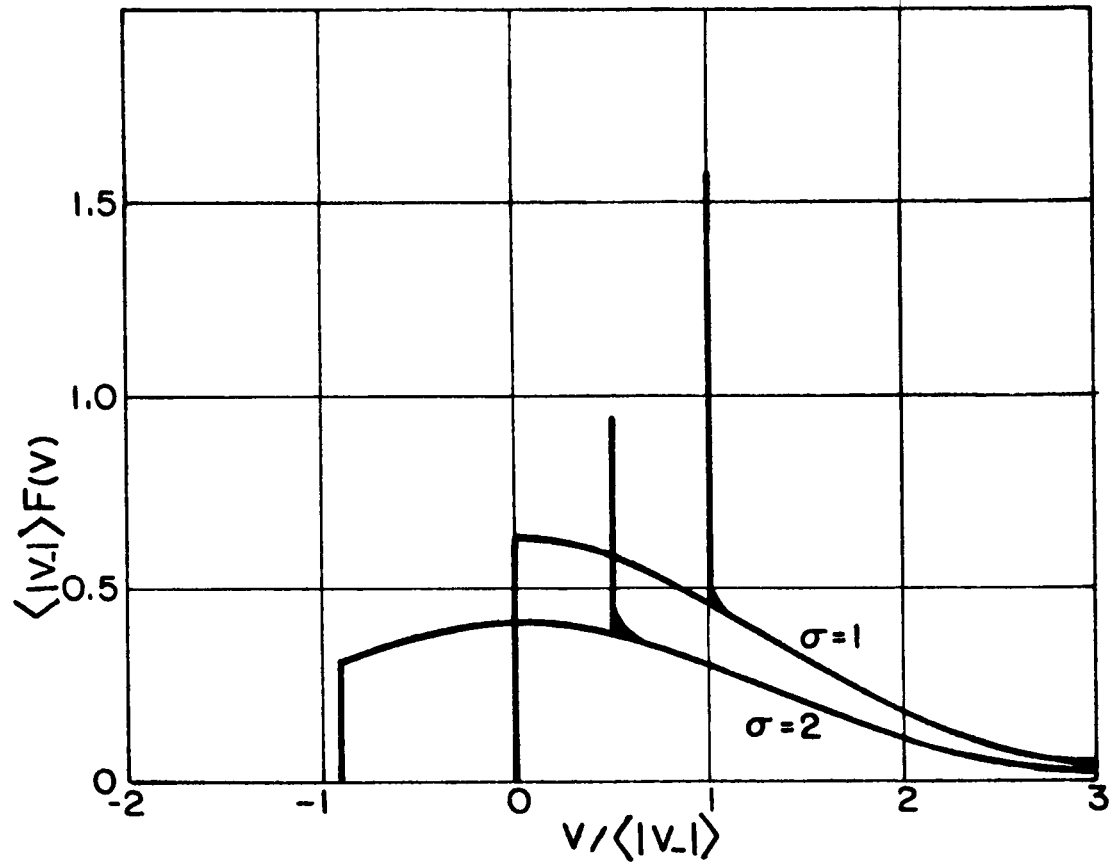


Fig. 11 Weighted Velocity-Distribution Function of
Electrons and Ions at Plasma Potential $\phi(b_2)$
for two velocity ratios $\sigma = \langle |v_-| \rangle / v_+(c_2)$.
Electron cutoff velocity for $\sigma = 2$ at $v_c = -0.913165 \langle |v_-| \rangle$
for $\sigma = 1$ at $v_c = 0$

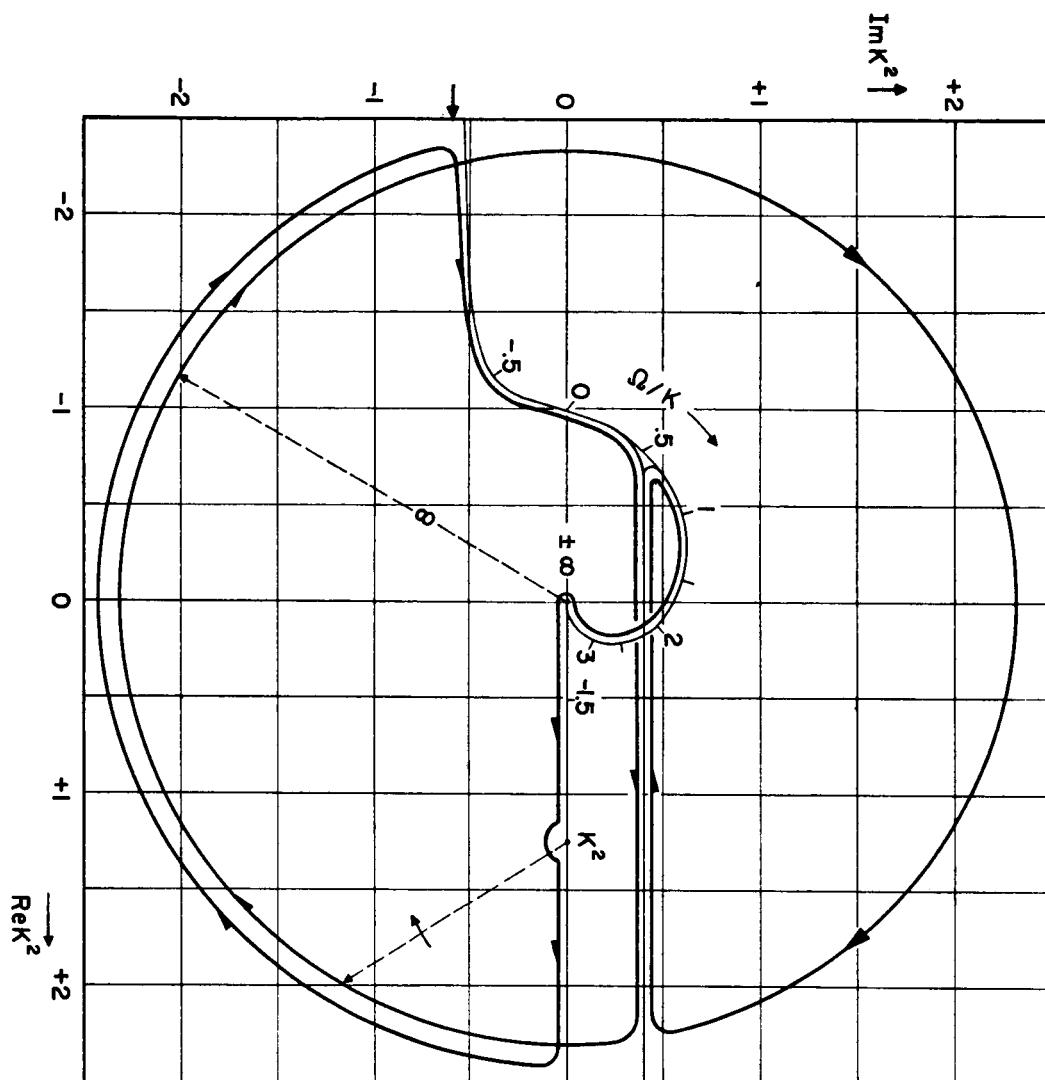


Fig. 12 Plasma Dispersion Function equ. (76)

for a Velocity Ratio $\sigma = \langle |v_-| \rangle / v_+(c_2) = 2$.

— wavenumber K as a function of real
wavevelocities Ω/K in normalized units

— wavenumber K for almost real
wavevelocities Ω/K , $\text{Im}\Omega = 0^-$, $K > 0$.

ion resonance at $\Omega/K = 0.5$

electron cutoff at $\Omega/K = -0.913165$

$$\text{Im}K^2 = -0.581339$$